# Carbonylhydridonitrosyltris(trimethylphosphine)molybdenum(0): An Activated Hydride Complex

Fupei Liang, Heiko Jacobsen, Helmut W. Schmalle, Thomas Fox, and Heinz Berke*

*Anorganisch-chemisches Institut, Universität Zürich, Winterthurerstrasse 190, CH-8057 Zürich, Switzerland*

*Received December 2, 1999*

The synthesis of the *mer*-Mo(CO)H(NO)($PMe_3$)$_3$ complex **3** is described, which is obtained from Mo(CO)$_4$(NO)$AlCl_4$ via the isolable intermediates MoCl(CO)(NO)($PMe_3$)$_3$ (**1**) and the borohydride complex Mo($\eta^1$-$BH_4$)(CO)(NO)($PMe_3$)$_3$ (**2**). The reactivity of **3** with respect to insertions has been probed. **3** thus reacts with benzaldehyde, benzophenone, acetophenone, and acetone to afford the corresponding alkoxide complexes Mo(CO)(NO)($PMe_3$)$_3$(OCHR′R″) (R′ = H, R″ = Ph (**4a**); R′, R″ = Ph (**4b**); R′ = Me, R″ = Ph (**4c**), and R′, R″ = Me (**4d**)). A high propensity of **3** to undergo carbonyl insertion was also manifested in its transformations with $CO_2$ and metal carbonyl compounds. The conversion of **3** with $CO_2$ leads to the formato-O-complex Mo(CO)(NO)($PMe_3$)$_3$(OCHO) (**5**), while CO induces $PMe_3$ substitution with formation of the nonisolable Mo(CO)$_2$(NO)($PMe_3$)$_2$H compound (**6**). Fe(CO)$_5$ readily inserts to yield the dinuclear formyl species ($Me_3P$)$_3$(ON)(OC)Mo($\mu$-OCH)Fe(CO)$_4$ (**7a**), and Re$_2$(CO)$_{10}$ is transformed to the related $\mu$-formyl complex ($Me_3P$)$_3$(ON)(OC)Mo($\mu$-OCH)Re$_2$(CO)$_9$ (**7b**) in an equilibrium reaction lying far to the formyl side. Temperature-dependent NMR measurements allowed us to derive equilibrium constants and $\Delta H = -46.5 \pm 0.6$ kJ/mol and $\Delta S = -103 \pm 2$ eu. These values for **7b** were approximately reproduced by accurate DFT calculations and investigated further via an incremental analysis of bond dissociation energies. Finally insertion reactions of **3** with various imines were studied. Only in the case of a bisdihydroproline ester did an insertion take place, however, across the ester carbonyl group. Concomitant elimination of a phosphine moiety was observed with formation of the isolable chelate complex *trans*-Mo[OCH(OCH$_3$)(C$_4$H$_6$N)](CO)(NO)($PMe_3$)$_2$ (**8**). The structures of complexes **2**, **3**, **4b**, **7a**, **7b**, and **8** were studied by X-ray diffraction.



Earlier it was shown that the strength of $L_nM-H$ bonds (M = transition metal) depends on the electronegativity of the M center.[1] Centers of low electronegativity cause weaker bonds to hydrogen and furthermore induce hydridic polarization of this ligand.[2]

In particular, our group has demonstrated that nitrosyl substitution may be used to effect lower orbital electronegativities[2] at various metal centers such as in the complexes *trans*-W(CO)$_2$H(NO)($PR_3$)$_2$,[3] Re(CO)H$_2$(NO)($PR_3$)$_2$,[4] and Mn,ReH(NO)$_2$($PR_3$)$_2$,[5] thus simulating early transition metal character.

Strongly $\sigma$-donating phosphine substituents and an increasing number of them are expected to enhance this effect, as demonstrated by a *trans*-W(CO)$_2$H(NO)($PR_3$)$_2$ series[3b,c] and the tris-substituted *mer*-W(CO)H(NO)($PMe_3$)$_3$ complex.[6] Phosphine-dependent hydridicities have also been traced in a Re(CO)$_n$H($PR_3$)$_{5-n}$ series.[7] On the basis of the fact that the radius and the electronegativity of molybdenum are smaller than those of tungsten, it can be inferred that the Mo−H bond in Mo(CO)$_{4-n}$(H)(NO)($PR_3$)$_n$ ($n$ = 2−4) complexes will still be weaker than the W−H bonds in analogous compounds, and therefore it is expected that the former display higher reactivity. With this background we decided to approach the synthesis of the tris(strong phosphine donor)-substituted molybdenum complex Mo(CO)H(NO)($PMe_3$)$_3$ and investigations of its reactivity. In this work, we succeeded in finding an appropriate synthetic access to this complex and tested its insertion behavior toward organic carbonyl groups, $CO_2$, CO, metal carbonyl moieties, and imines.

(1) (a) Labinger, J. A.; Bercaw, J. E. *Organometallics* **1988**, *7*, 926. (b) Nolan, S. P.; Stern, D., Marks, T. J. *J. Am. Chem. Soc.* **1989**, *111*, 7844. (c) Marks, T. J. *Bonding Energetics in Organometallic Compounds*; ACS Symposium Series 428; American Chemical Society: Washington, DC, 1990.

(2) Berke, H.; Burger, P. *Comments Inorg. Chem.* **1994**, *16*, 279.

(3) (a) Kundel, P.; Berke, H. *J. Organomet. Chem.* **1987**, *335*, 353. (b) van der Zeijden, A. A. H.; Sontag, C.; Bosch, H. W.; Shklover, V.; Berke, H.; Nanz, D.; von Philipsborn, W. *Helv. Chim. Acta* **1991**, *74*, 1194. (c) van der Zeijden, A. A. H.; Bosch, H. W.; Berke, H. *Organometallics* **1992**, *11*, 2051. (d) van der Zeijden, A. A. H.; Berke, H. *Helv. Chim. Acta* **1992**, *75*, 513.

(4) (a) Messmer, A.; Jacobsen, H.; Berke, H. *Chem. Eur. J.* **1999**, *5*, 3341. (b) Jacobsen, H.; Heinze, K.; Llamazares, A.; Schmalle, H. W.; Artus, G.; Berke, H. *J. Chem. Soc. Dalton Trans.* **1999**, 1717. (c) Gusev, D. G.; Llamazares, A.; Artus, G.; Berke, H. *Organometallics* **1999**, *18*, 75. (d) Nietlispach, D.; Bosch, H. W.; Berke, H. *Chem. Ber.* **1994**, *127*, 2403. (e) Nietlispach, D.; Bakhmutov, V. I.; Berke, H. *J. Am. Chem. Soc.* **1993**, *115*, 9191.

(5) (a) Belkova, N. V.; Shubina, E. S.; Ionidis, A. V.; Epstein, L. M.; Jacobsen, H.; Messmer, A.; Berke H. *Inorg. Chem.* **1997**, *36*, 1522. (b) Hund, H. U.; Ruppli, U.; Berke, H. *Helv. Chim. Acta* **1993**, *76*, 963.

(6) Bäth, F. Ph.D. Thesis, University of Zurich, 1998. Höck, J.;Fox, T.; Schmalle, H.; Berke, H. *Chimia* **1999**, *53*, 350.

(7) (a) Gusev, D. G.; Nietlispach, D.; Eremenko, I. L.; Berke, H. *Inorg. Chem.* **1993**, *32*, 3628. (b) Nietlispach, D.; Veghini D.; Berke, H. *Helv. Chim. Acta* **1994,** *77*, 2197.

10.1021/om990945t CCC: $19.00 
Publication on Web 04/14/2000

**Scheme 1**

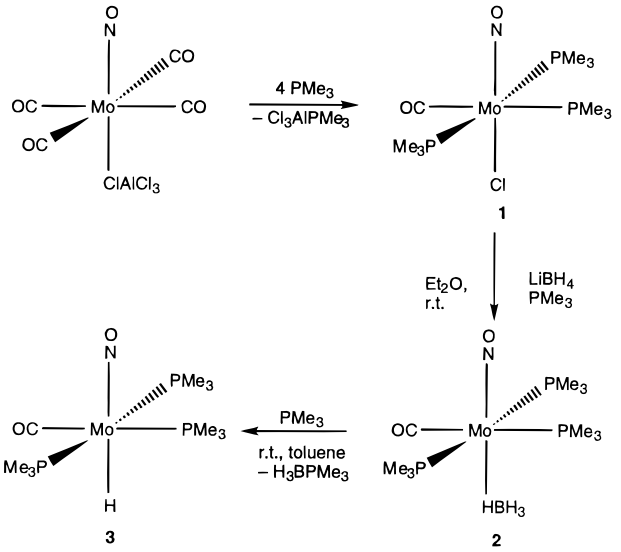


## Results and Discussions

**1. Synthesis of *mer*-Mo(CO)H(NO)($PMe_3$)$_3$ (3).** Hillhouse et al. have reported the preparation of *mer*-Mo(CO)H(NO)($PMePh_2$)$_3$ via a direct reaction of *mer*-Mo(Cl)(CO)(NO)($PMePh_2$)$_3$ with $LiBH_4$ and $PMePh_2$ in THF.[8] Access to the analogous chloride Mo(Cl)(CO)(NO)-($PMe_3$)$_3$ (**1**) has been achieved by an autoclave reaction of Mo($AlCl_4$)(CO)$_4$(NO), prepared according to a literature procedure.[9] Conversion of it with 4 equiv of $PMe_3$ in THF at 80 °C led to **1** in 71% yield. The structure and composition of **1** have been established by IR, NMR, and elemental analysis. The $^1$H NMR in $C_6D_6$ shows a triplet at 1.25 ppm and a doublet at 1.06 ppm, and in the $^{31}$P NMR a doublet at $\delta = -10.3$ ppm and a triplet at $-17.5$ ppm ($^2J_{PP} = 30$ Hz) were observed. Both resonance patterns are in accord with the meridional disposition of three phosphine ligands.

Compound **1** could not directly be transformed into **3** by $LiBH_4$ in $Et_2O$. At room temperature this reaction produced the borohydride complex Mo(CO)($HBH_3$)(NO)-($PMe_3$)$_3$ (**2**), instead. Conversion of **2** with $PMe_3$ in toluene at room temperature then gave the hydride **3** (Scheme 1).

The $^1$H NMR spectrum of **2** reveals a broad quartet at $\delta$ $-1.51$ ppm with a characteristic $^{11}$B coupling ($^2J_{HB}$ = 86.2 Hz), which was therefore assigned to the protons of the $BH_4$ group. The spectrum furthermore displays a triplet at 1.19 ppm ($^2J_{HP} = 3.2$ Hz) and a broad signal at 1.03 ppm, both of which belong to the $Me_{phosphine}$ residues. The broadness of the latter signal can most likely be attributed to interference of boron quadrupolar relaxation. A similar picture is obtained by $^{31}$P NMR. In the spectrum one resonance at $-17.4$ ppm also appears broadened, again explained on the basis of boron coupling. This observation is in agreement with previous ones on related boron-containing compounds.[10] The other $^{31}$P NMR signal, a singlet at $-10.3$ ppm, is assigned to the trans-disposed phosphorus ligands. At low temperature ($-40$ °C) further splitting of the signal pattern can be observed: The $^1$H NMR ($C_6D_5CD_3$) spectrum shows a triplet at $\delta$ 1.15 ppm and a doublet at $\delta$ 0.93 ppm, and the $^{31}$P NMR displays splitting into a doublet at $\delta$ $-10$ ppm and a triplet at $\delta$ $-16.0$ ppm ($^2J_{PP} = 28$ Hz). The fact that the $^{11}$B NMR spectrum shows a quintet at $\delta$ $-38.5$ ppm ($^2J_{HB} = 85$ Hz) confirms the presence of the $BH_4$ unit in the molecule. It has however to be assumed that all four hydrogen signals get averaged by a dynamic process fast on the NMR time scale. The $\eta^1$ binding of the $BH_4$ moiety has finally been assured by an X-ray diffraction study.

Treatment of **2** with 15 equiv of $PMe_3$ in toluene at room temperature yielded the hydride **3**. It is noteworthy that this reaction requires a large excess of $PMe_3$ and a relatively long reaction time of 2 days. It has been found that when cyclic amines are used for the $BH_3$ scavenging, stoichiometric amounts of the agent may be sufficient for complete conversion and an even shorter reaction time may be applied. For instance, NMR monitoring showed that the conversion of **2** with quinuclidine or piperidine required only 1 equiv of the amine and 10 h. However, despite these advantages, it rendered finally to be very difficult to remove in these cases the $R_3N \rightarrow BH_3$ byproducts from **3**, so that these routes could not be pursued further.

The $^1$H NMR spectrum of **3** shows among other resonances that of the hydride ligand. It appears as a doublet of triplets at $\delta$ $-1.92$ ppm, a characteristic pattern of cis-coupling with three meridionally disposed $PMe_3$ substituents. The structure of **3** has finally inequivocally been established by an X-ray diffraction study, which will be discussed later.

In the room-temperature IR spectrum of **3**, as well as in the solid-state Raman spectrum, only one superimposed band appears for $\nu$(NO) and $\nu$(MoH). In contrast to this, the low-temperature IR spectrum in hexane taken at $-70$ °C displays two bands around 1600 cm$^{-1}$, which are assigned to $\nu$(MoH) (1609 cm$^{-1}$) and $\nu$(NO) (1596 cm$^{-1}$). The position of the $\nu$(MoH) band at very low vibrational energies allows one to conclude that the Mo−H bond of **3** is relatively weak, which is also mirrored in the relatively small calculated BDE given later.

**2. Insertion Reactions of 3.** As indicated before, insertion reactions into a M−H bond naturally depend on the M−H bond strength, and since we expected the Mo−H bond of **3** to be on the weak side of the thermodynamic scale, it was anticipated that **3** would show an increased tendency to react with aldehydes and ketones. In fact, it was seen earlier for the presumably quite strong Ir−H bond that deinsertions of organic carbonyl compounds are preferred; that is, the corresponding alkoxides decompose at room temperature with $\beta$-H-elimination.[12] It should furthermore be noted that we have experienced earlier that the insertion reaction of *trans*,*trans*-W(CO)$_2$H(NO)($PMe_3$)$_2$ with benzaldehyde afforded an alkoxide. However, this complex turned out to be unstable with respect to loss of CO due to the cis-labilizing effect of the alkoxide group.[13] In contrast to this behavior, we expected similar alkoxide

(8) Cheng, T.-Y.; Southern, J. S.; Hillhouse, G. L. *Organometallics* **1997**, *16*, 2335
(9) Seyferth, K.; Taube, R. *J. Organomet. Chem.* **1982**, 229, 275.
(10) (a) Beall, H.; Bushweller, C. H. *Chem. Rev.* **1973**, *73*, 465. (b) Marks, T. J.; Kolb, J. R. *Chem. Rev.* **1977**, *77*, 263.
(11) Jacobsen, H.; Jonas, V.; Werner, D.; Messmer, A.; Panitz, J.-C.; Berke, H.; Thiel, W. *Helv. Chim. Acta* **1999,** *82*, 297.
(12) Blum, O.; Milstein, D. *J. Am. Chem. Soc.* **1995**, *117*, 4582.
(13) Van der Zeijden, A. A. H.; Bosch, H. W.; Berke, H. *Organometallics* **1992**, *11*, 2051

**Scheme 2**

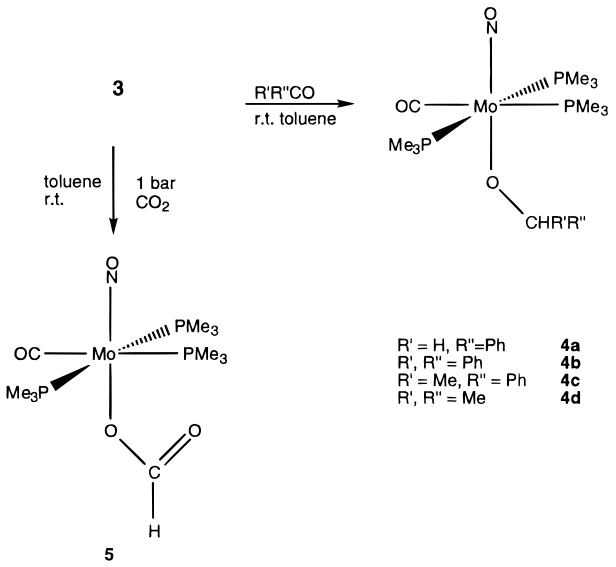


derivatives with a reduced content of labile CO to be quite stable, and indeed the reaction of **3** with PhCHO produced a stable benzyloxy species **4a** (Scheme 2).

The reaction proceeded smoothly at room temperature in toluene and was completed within a few minutes. **4a** can be isolated in 87% yield as analytically pure yellow crystals. The $^1$H NMR spectrum in $C_6D_6$ shows, among other resonances, a characteristic signal at $\delta$ 4.91 ppm, and the $^{13}C\{^1H\}$NMR spectrum displays a doublet of triplets at $\delta$ 75.5 ppm, both of which signals correspond to the resonances of the newly formed $CH_2$ moiety involving coupling with the three $PMe_3$ ligands. In unique reaction steps aldehydes and ketones have only rarely been demonstated to insert into transition metal hydrogen bonds.[3c,d,14] Furthermore, ketones are normally even more reluctant to undergo these transformations. Such insertions, however, have been invoked as key steps in catalytic reduction with transition metal compounds.[15] We therefore tried to explore the possibility of insertions of **3** with typical simple ketones and found that these take place with benzophenone, acetophenone, and acetone to afford complexes **4b**−**d** in significantly slower reactions than those with benzaldehyde (Scheme 2). For acetone as the most reluctant reagent in this series a higher stoichoimetric ratio of 1:2 had to be applied; in the other cases a 1:1 ratio in toluene revealed at room temperature somewhat faster rates of these presumably second-order processes. Under the given conditions the conversions took approximately 3 h for benzophenone, 7 h for acetophenone, and 10 h for acetone. The phenyl substituent apparently facilitates these reactions via enhanced electrophilicity of the $C_{carbonyl}$ atom.

In the $^1$H and $^{13}$C NMR spectra of the compounds **4b**−**d** characteristic resonances of the newly formed −CH− moieties appear. In $C_6D_6$ **4b** displays for this group a singlet at $\delta$ 5.55 ppm ($^1$H NMR) and a doublet of triplets at $\delta$ 87.4 ppm ($^{13}C\{^1H\}$ NMR). The splitting of the latter signal is assigned to the coupling with the phosphorus nuclei. In the $^1$H NMR spectrum of **4c** a quartet appears at $\delta$ 4.62 ppm, which results from the coupling of the methyne proton with those of the methyl group. Similarily the CH proton of **4d** couples with the two methyl groups, showing a heptet at $\delta$ 3.75 ppm ($^3J_{HH}$ = 6 Hz). In the $^{13}C\{^1H\}$ NMR spectra of both **4c** and **4d** the CH groups are attributed to a doublet of triplet resonances at $\delta$ 79.1 and 70.7 ppm, respectively, which appear as pseudo-quintets due to partial overlap of the splitting patterns. It is noteworthy that the trans phosphine ligands in complex **4c** are diastereotopic. This is caused by the presence of a chiral carbon atom in the alkoxy residue. Therefore, the $^1$H NMR spectrum of the phosphine ligands in **4c** consists of three sets of signals at $\delta$ 1.28, 1.11, and 1.03 ppm, respectively. The $^{31}P\{^1H\}$ NMR spectrum of **4c** does not reflect this diastereotopy. Comparable to the spectra of **4b** and **4d** only two groups of signals are present, a doublet at $\delta$ −12.3 and a triplet at $\delta$ −17.5 ppm. In an exemplary way, **4b** could be characterized by an X-ray diffraction study.

Insertions of $CO_2$ into a metal hydride bond are of growing interest, since they are assumed to be the initial steps in the hydrogenation of $CO_2$.[16] Therefore, we tested whether hydride **3** would be activated enough to undergo such a transformation.

Indeed, reaction of **3** with 1 bar $CO_2$ in toluene afforded at room temperature the formato-O-complex **5** (Scheme 2), which can be isolated in 85% yield as analytically pure yellow crystals after recrystallization from pentane. In the $^1$H NMR spectrum **5** shows a characteristic quartet type signal at $\delta$ 8.59 ppm, which is assigned to the formate proton. Apparently, the three P nuclei behave in this case as magnetically equivalent. In the $^{13}C\{^1H\}$ NMR spectrum the $^{13}$C resonance of the $C_{formato}$ atom is observed as a multiplet at 167.1 ppm. The other $^1$H and $^{13}$C NMR resonances of **5** are similar to those of **3**, which suggests closely related carbonyl and phosphine frameworks for these complexes. The IR spectrum of **5** in hexane shows a pattern similar to that of *mer*-W(OCHO)(CO)(NO)$(PMe_3)_3$.[6] Among others it consists of an intense $\nu$(NO) band at 1609 cm$^{-1}$ and a $\nu$(OCO) band at 1625 cm$^{-1}$. [3a] The expected $\nu$(CO) absorption is split in the solid-state spectrum, revealing bands at 1958 and 1931 cm$^{-1}$.

The migratory insertion of CO into a metal−hydride bond to produce a formyl species has been proposed as a key step in the homogeneous catalytic hydrogenation of CO.[17] However, the model type isolated insertion step

(14) Selected references: (a) Grey, R. A.; Pez, G. P.; Wallo, A. *J. Am. Chem. Soc.* **1981**, *103*, 7536. (b) Gaus, P. L.; Kao, S. C.; Youngdahl, K.; Darensbourg, M. Y. *J. Am. Chem. Soc.* **1985**, *107*, 2428. (c) Tooley, P. A.; Ovalles, C.; Kao, S. C.; Darensbourg, D. J.; Darensbourg, M. Y. *J. Am. Chem. Soc.* **1986**, *108*, 5465. (d) Debad, J. D.; Legzdins, P.; Lumb, S. A.; Batchelor, R. J.; Einstein, F. W. B. *Organometallics* **1995**, *14*, 2543. (e) Van Leeuwen, P. W. N. M.; Roobeek, C. F.; Orpen, A. G. *Organometallics* **1990**, *9*, 2179.

(15) Selected references: (a) Ponec, V. *Catal. Rev.-Sci. Eng.* **1978**, *18*, 151 (b) Costa, L. C. *Catal. Rev. Sci. Eng.* **1983**, *25*, 325. (c) Noyori, R.; Takaya, H. *Acc. Chem. Res.* **1990**, *23*, 345. (d) Burk, M. J.; Gross, M. F.; Harper, T. G. P.; Kalberg, C. S.; Lee, J. R.; Martinez, J. P. *Pure Appl. Chem.* **1996**, *68*, 37. (e) Jiang, Q.; Jiang, Y.; Xiao, D.; Cao, P.; Zhang, X. *Angew. Chem.* **1998**, *110*, 1203. (f) Nomura, K. *J. Mol. Catal. A: Chem.* **1998**, *130*, 1. (g) Kvintovics, P.; Bakos, J.; Heil, B. *J. Mol. Catal.* **1985**, *32*, 111. (h) Palmer, M. J.; Wills, M. *Tetrahedron: Asymmetry* **1999**, *10*, 2045.

(16) (a) Leitner, W. *Angew. Chem., Int. Ed. Engl.* **1995**, *34*, 2207. (b) Gibson, D. H. *Chem. Rev.* **1996**, *96*, 2063. (c) Toyohara, K.; Nagao, H.; Mizukawa, T.; Tanaka, K. *Inorg. Chem.* **1995**, *34*, 5399. (d) Cutler, A. R.; Hanna, P. K.; Vites, J. C. *Chem. Rev.* **1988**, *88*, 1363. (e) Darensbourg, D. J.; Kudaroski, R. A. *Adv. Organomet. Chem.* **1983**, *22*, 129. (f) Darensbourg, D. J.; Ovalles, C. *Chemtech* **1985**, *15*, 636. (g) Darensbourg, D. J.; Ovalles, C. *J. Am. Chem. Soc.* **1987**, *109*, 3330. (h) Darensbourg, D. J.; Darensbourg, M. Y.; Goh, L. Y.; Ludvig, M.; Wiegreffe, P. *J. Am. Chem. Soc.* **1987**, *109*, 7539.

**Scheme 3**

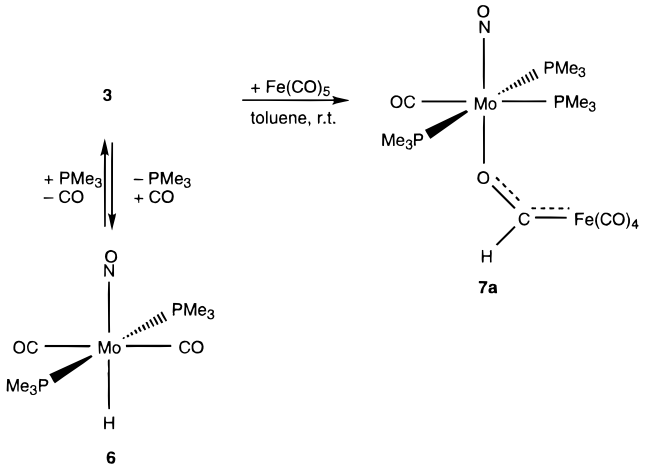


**Scheme 4**

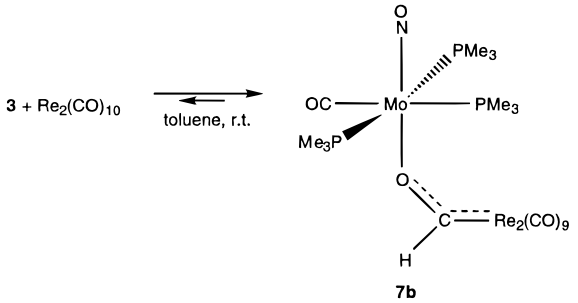


of CO into the M−H bond remains a rarity,[18] presumably due to the high bond energy of CO. Considering the reactivity of **3** and its indicated weaker Mo−H bond, we set out to investigate the insertion ability of the Mo−H bond of **3** with regard to CO. At first, the reaction of **3** with 1 bar CO was studied, which however led merely to substitution of the unique phosphine ligand to form complex **6** (Scheme 3). The reaction turned out to be an equilibrium, which caused reversal of the reaction during the necessary removal of the solvent in vacuo, and this thus prevented isolation and full characterization of **6**. But the existence of compound **6** can clearly be deduced from the $^1$H NMR spectrum, in which a triplet at −2.73 ppm ($^2J_{PH}$ = 29.6 Hz) corresponding to the $H_{Mo}$ ligand is observed. Another triplet at 1.12 ppm ($^2J_{PH}$ = 3.2 Hz) was assigned to the protons of the phosphine ligands. In accord with the proposed structure of **6**, the $^{31}$P{$^1$H} NMR spectrum revealed a singlet at −6.5 ppm. The observation that substitution took place may imply that the direct insertion of CO into the Mo−H bond is a still thermodynamically unfavorable process. To possibly overcome any of these factors, we then attempted reaction of **3** with CO bound in metal carbonyl compounds, such as $Fe(CO)_5$ and $Re_2(CO)_{10}$.

Treatment of **3** with 1 equiv of $Fe(CO)_5$ indeed produced at room temperature in toluene the formyl-bridged complex **7a** (Scheme 3), which was isolated as yellow crystals in 88% yield after recrystallization from pentane. The bridging formyl group of **7a** gives rise to characteristic NMR resonances. In the $^1$H NMR spectrum ($C_6D_6$) one finds a singlet at 14.09 ppm for the $H_{formyl}$ nucleus, and in the $^{13}$C{$^1$H} NMR spectrum one observes a quartet at 306.1 ppm for the $C_{formyl}$ atom. The chemical shift of the $H_{formyl}$ proton appears in the range of that of $[Fe(CO)_4CHO]^-$ (15.0 ppm) reported by Collman et al.[19] However, the $^{13}$C chemical shift of the $C_{formyl}$ atom is observed considerably (about 26.0 ppm) downfield from that of $[Fe(CO)_4CHO]^-$, which is attributed to an efficient electron withdrawl in the bridging coordination mode. The IR spectrum of **7a** shows, besides $\nu$(NO) and $\nu$(CO) of the Mo-coordinated ligands at 1619 and 1931 cm$^{-1}$, three bands at 2035 (m), 1952 (m), 1925 (s) cm$^{-1}$, which are assigned to the $\nu$(CO) vibrations of the $Fe(CO)_4$ unit. This absorption pattern resembles closely that of the "parent" $[Fe(CO)_4CHO]^-$ complex.[19]

**3** can also react with $Re_2(CO)_{10}$ in toluene to generate the bridging formyl compound **7b** (Scheme 4). However, in contrast to the reaction with $Fe(CO)_5$, the reaction with $Re_2(CO)_{10}$ is an equilibrium lying at room temperature considerably to the right side (**3**:$Re_2(CO)_{10}$ = 1:1, 0.051 mol/L, room temperature, $K$ = 560 L/mol), as determined by NMR spectroscopy. Despite the equilibrium situation of its formation, **7b** can be isolated as analytically pure orange crystals in 80% yield after recrystallization from $Et_2O$. In the $^1$H NMR spectrum of **7b** the proton resonance of the formyl group is found at 15.07 ppm, which is close to that of $[Re_2(CO)_9(CHO)]^-$.[20] The $^{13}$C{$^1$H} NMR spectrum also demonstrates the presence of a $C_{formyl}$ atom displaying a pseudo-quartet at 302.3 ppm. The $^{13}$C chemical shift of the bridging formyl carbon atom of **7b** is downfield to that of $[Re_2(CO)_9(CHO)]^-$.[20]

The temperature dependence of $K$ allowed the calculation of $\Delta H = -46.5 \pm 0.6$ kJ/mol and $\Delta S = -103 \pm 2$ eu for the association reaction (see van't Hoff plot Figure 1). Apparently the hydride transfer from **3** onto $Re_2(CO)_{10}$ is moderately exothermic, reflecting a weak Mo−H bond and the relative strength of the newly installed C−H and Mo−O bonds (see DFT calculations vide supra). The significantly negative $\Delta S$ is in agreement with the associative character of the process.

It was expected that complexes **7a** and **7b** would react further with an excess of **3**. We have therefore at-

(17) (a) Miller, R. L.; Toreki, R.; La Pointe, R. E.; Wolczanski, P. T.; Van Duyne, G. D.; Roe, D. C. *J. Am. Chem. Soc.* **1993**, *115*, 5570, and references therein. (b) Gladysz J. A. *Adv. Organomet. Chem.* **1982,** *20*, 1. (c) Burckhardt, U.; Tilley, T. D. *J. Am. Chem. Soc.* **1999**, *121*, 6328. (d) Herrmann, W. A. *Angew. Chem., Int. Ed. Engl.* **1982**, *21*, 117. (e) Blackborow, J. R.; Daroda, R. J.; Wilkinson, G. *Coord. Chem. Rev.* **1982**, *43*, 17. (f) Masters, C. *Adv. Organomet. Chem.* **1979**, *17*, 61. (g) Klingler, R. J.; Rathke, J. W. *Progr. Inorg. Chem.* **1991**, *39*, 113. (h) Simpson, M. C.; ColeHamilton, D. J. *Coord. Chem. Rev.* **1996**, *155*, 163. (i) Süss-Fink, G.; Meister, G. *Adv. Organomet. Chem.* **1993**, *35*, 41. (k) Dombeck, B. P. *Adv. Catal.* **1983**, *32*, 325. (l) Marko, L. *Trans. Met. Chem.* **1992**, *17*, 474. (m) Ford, P. C. *Catalytic Activation of Carbon Monoxide;* ACS Symposium Series 152; American Chemical Society: Washington, DC, 1981.

(18) (a) Fagan, P. J.; Moloy, K. G.; Marks, T. J. *J. Am. Chem. Soc.* **1981**, *103*, 6959. (b) Wayland, B. B.; Woods, B. A. *J. Chem. Soc., Chem. Commun.* **1981**, 700. (c) Wei M. L.; Wayland B. B. *Organometallics* **1996**, *15*, 4681. (d) Wayland, B. B.; Coffin, V. L.; Sherry, A. E.; Brennen, W. R. *ACS Symp. Ser.* **1990**, *428*, 148. (e) Wayland B. B.; Sherry A. E.; Poszmik G.; Bunn A. G. *J. Am. Chem. Soc.* **1992**, *114*, 1673. (f) Burckhardt U.; Tilley T. D. *J. Am. Chem. Soc.* **1999**, *121*, 6328. (g) Wolczansky P. T.; Threlkel R. S.; Bercaw J. E. *J. Am. Chem. Soc.* **1978**, *101*, 218. (h) Labinger J. A.; Wong K. S. *ACS Symp. Ser.* **1981**, *152*, 253. (i) Erker, G.; Schmuck, S.; Hoffmann, U. *J. Am. Chem. Soc.* **1991**, *113*, 2330. (k) Kropp, K.; Skribbe, V.; Erker, G.; Krüger, C. *J. Am. Chem. Soc.* **1983**, *105*, 3353. (l) Fryzuk, M. D.; Mylvaganam, M.; Zaworotko, M. J.; MacGillivray, L. R. *Organometallics* **1996**, *15*, 1134. (m) Rappe, A. K. *J. Am. Chem. Soc.* **1987,** *109*, 5605, and references therein.

(19) Collman, J. P.; Winter, S. R. *J. Am. Chem. Soc.* **1973**, *95*, 4089.

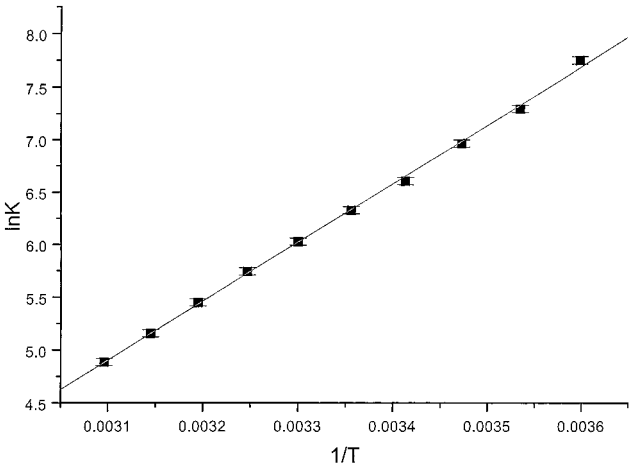


**Figure 1.** Van't Hoff plot for the equilibrium reaction of **3** with $Re_2(CO)_{10}$ according to Scheme 4.

tempted their reaction with 3 equiv of **3** under various conditions, but no further transformation could be observed.

In view of the high hydride activity of **3**, we also sought to investigate its insertion capability toward imines. The insertion of imines into transition metal hydrides is of great general importance, since it is assumed to be the initial step in catalytic hydrogenations of imines generating amines.[15g,21] Imines as hetero-olefins generally appear to be quite reluctant in reactions with $L_nM-H$ bonds, indicated by the fact that they require very activated transition metal hydrides especially in cases when the insertions are observable as isolated steps.[14d,21a]

From the series of imines PhN=CHPh, MeN=CHPh, and $Ph_2C$=NH, the latter two did not react under various conditions, varying the stoichiometric ratios, temperatures, and reaction times. Only PhN=CHPh was found to be converted to a new product at 60 °C, which unfortunately could not be isolated, and by this circumstance the structure of this reaction product could not be assigned.

Considering the lower reactivity of the given imine series with **3**, we turned to applying an activated imine. The reaction between **3** and a bisdihydroproline derivative was prototypically investigated (Scheme 5). Insertion indeed occurred, however, not into the C=N double bond of the imine but rather into the C=O bond of the ester group and at the same time subsequent loss of a phosphine ligand took place with formation of an O,N-chelated product **8** (Scheme 5). Complex **8** was isolated in 83% yield as analytically pure red crystals and fully characterized by elemental analysis, NMR, IR, MS, and an X-ray diffraction study.

The $^1H$ NMR spectrum of **8** ($C_6D_6$) shows a triplet at $\delta$ 5.41 ppm, and the $^{13}C\{^1H\}$ NMR spectrum reveals a singlet at 104. 9 ppm, both of which are assigned to the

**Scheme 5**

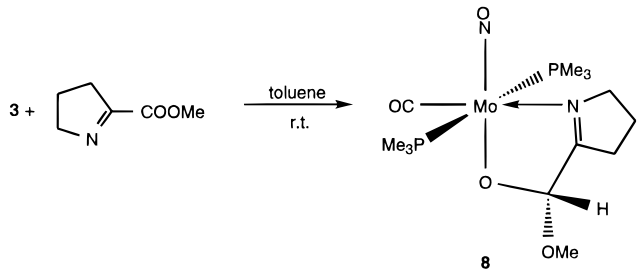


respective $^1H$ and $^{13}C$ nuclei of the $-OC(H)O-$ group. The $^{13}C$ signal of the C=N group is observed at 186.3 ppm, which is shifted considerably downfield with respect to that of the free imine ($\Delta\delta$ 22.5 ppm). This can be attributed to the coordination of the $N_{imine}$ atom. The two phosphine ligands in **8** are inequivalent due to the presence of a chiral carbon atom in the molecule, which is seen from the $^1H$ and $^{31}P$ resonances of the phosphine ligands, giving rise to two sets of signals at 1.19 and 1.03 ppm in the $^1H$ NMR and at −6.1 and −6.2 ppm in the $^{31}P$ NMR spectra.

The reaction according to Scheme 5 was conceived to proceed via an intermediate. Therefore, a more detailed NMR study of the reaction was carried out at low temperature in order to trace such a species. However, no intermediate was detected and **8** appeared as the sole product, even at the relatively low temperature of −20 °C where the reaction still proceeded. This suggests that the displacement reaction of $PMe_3$ takes place practically simultaneously with the insertion reaction.

**Thermodynamic Considerations of the Metal Carbonyl Insertion Reaction with 3 Applying DFT Calculations.** DFT calculations allowed for a partitioning of the equilibrium reaction of Scheme 4 into respective bond increments. Our computational approach has been used before in studying the thermodynamic properties of the transition metal hydride bond,[22a] and the results were in good agreement with experimental values.[22b] These calculations validate the DFT scheme applied in our analysis. The following thermodynamic cycle based on homolytic bond cleavage reactions in the gas phase has been considered to arrive at a theoretical estimate for the enthalpy of the reaction of **3** with $Re_2(CO)_{10}$:

$$\mathbf{3} \rightarrow [Mo(CO)(NO)(PMe_3)_3]^\bullet + H^\bullet \qquad \Delta H = 296 \text{ kJ/mol} \quad \text{(I)}$$

$$Re_2(CO)_{10} + H^\bullet \rightarrow [Re_2(CO)_9(CHO)]^\bullet \qquad \Delta H = -63 \text{ kJ/mol} \quad \text{(II)}$$

$$[Mo(CO)(NO)(PMe_3)_3]^\bullet + [Re_2(CO)_9(CHO)]^\bullet \rightarrow \mathbf{7b} \qquad \Delta H = -268 \text{ kJ/mol} \quad \text{(III)}$$

The Mo−H bond strength amounts to 296 kJ/mol, and the $H$ affinity of $Re_2(CO)_{10}$, −62 kJ/mol, is somewhat lower than that of carbon monoxide ($\Delta H = -75$ kJ/mol).[23] For the insertion reaction into the metal−hydride bond the reaction sequence affords a value of $\Delta H = -34$ kJ/mol, which is in fair agreement with the experimental result.

(20) Casey C. P.; Neumann S. M. *J. Am. Chem. Soc.* **1978**, *100*, 2544.
(21) Selected references: (a) Willoughby, C. A.; Buchwald, S. L. *J. Am. Chem. Soc.* **1994**, *116*, 8952. (b) Obora, Y.; Ohta, T.; Stern, C. L.; Marks, T. J. *J. Am. Chem. Soc.* **1997**, *119*, 3745. (c) Christensen, N. J.; Hunter, A. D.; Legzdins, P.; Sánchez, L. *Inorg. Chem.* **1987**, *26*, 3344. (d) Kobayashi, S.; Ishitani, H. *Chem. Rev.* **1999**, *99*, 1069. (e) Ringwald, M.; Sturmer, R.; Brintzinger, H. H. *J. Am. Chem. Soc.* **1999**, *121*, 1524. (f) James, B. R. *Catal. Today* **1997**, *37*, 209. (g) Blaser, H. U.; Spindler, F. *Top. Catal.* **1997**, *4*, 275. (h) Schnider, P.; Koch, G.; Pretot, R.; Wang, G. Z.; Bohnen, F. M.; Krüger, C.; Pfaltz, A. *Chem. Eur. J.* **1997**, *3*, 887.

(22) (a) Folga, E.; Ziegler, T. *J. Am. Chem. Soc.* **1993**, *115*, 5169. (b) Simoes, J. A. M.; Beauchamp, J. L. *Chem. Rev.* **1990**, *90*, 629.
(23) Kerr, J. A. *Chem. Rev.* **1966**, *66*, 465.

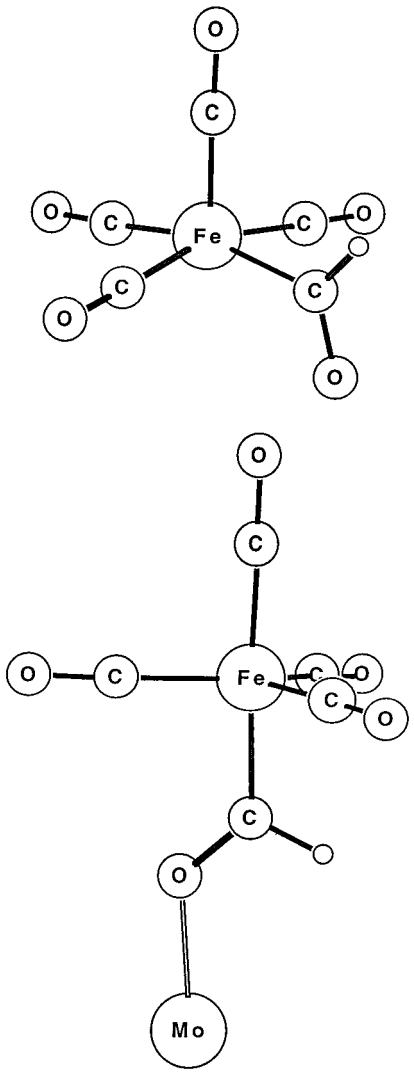


**Figure 2.** Optimized geometries for $[Fe(CO)_4(CHO)]^-$ and $Mo(CO)(PMe_3)_3(NO)OCHFe(CO)_4$ (**7a**). The phosphine, the carbonyl, and the nitrosyl ligands at Mo have been omitted for clarity.

We have also considered the reaction of **3** with $Fe(CO)_5$, as shown in Scheme 3. Reaction eq I, together with eqs IV and V, allows the calculation of $\Delta H$ for this conversion:

$$Fe(CO)_5 + H^\bullet \rightarrow [Fe(CO)_4(CHO)]^\bullet \qquad \Delta H = -105 \text{ kJ/mol} \quad \text{(IV)}$$

$$[Mo(CO)(NO)(PMe_3)_3]^\bullet + [Fe(CO)_4(CHO)]^\bullet \rightarrow \mathbf{7a} \qquad \Delta H = -220 \text{ kJ/mol} \quad \text{(V)}$$

For the formation of **7a** a reaction enthalpy of $\Delta H = -29$ kJ/mol is obtained. This value is similar to that of **7b**, although the reaction of **3** with $Fe(CO)_5$ is not at equilibrium at room temperature. The difference between the formation of **7a** and **7b** might be understood when the bond-breaking and bond-making steps are separately analyzed. It is noticeable that the iron carbonyl has a much higher hydrogen affinity than the rhenium carbonyl (compare eqs IV and II). The structure of this interesting radical resulting from reaction eq IV is displayed in Figure 2.

Unlike the anion $[Fe(CO)_4(CHO)]^-$, which derives its structure from a trigonal bipyramide with the formyl ligand occupying an axial position,[24] $[Fe(CO)_4(CHO)]^\bullet$ possesses a square pyramidal coordination, with the HCO ligand occupying one of the basal positions. The spin density is mainly localized on the metal center. If this fragment is combined with the $[Mo(CO)(NO)(PMe_3)_3]^\bullet$ to form **7a**, the iron fragment rearranges to adapt a trigonal bipyramidal coordination, as shown in Figure 2. The situation is different when the reaction with dirhenium decacarbonyl is considered. Although the most stable geometry we have found for $[Re_2(CO)_9(CHO)]^\bullet$ results from hydrogen transfer to a carbonyl group in axial position, the isomer with equatorial HCO also represents a local minimum on the energy surface and is only 17 kJ/mol higher in energy. Its geometry is closely related to that of the Re fragment in **7b**. The spin density is to a large part localized on the formyl oxygen atom, which in turn will form the bond to the Mo radical. If the insertion into the Mo−H bond takes place via a hydrogen transfer step, the required rearrangement of the iron fragment might explain why the formation of **7a** is not an equilibrium reaction. The dissociation of **7a** into the two radical fragments is likely to have a higher kinetic barrier than the dissociation of **7b**. In the former case, bond breaking does not directly lead to minimum structures but is associated with a rearrangement of the formyl radical.

We also considered possible heterolytic bond cleavage reactions. The key steps, which are associated with the hydride affinity of the metal carbonyls, are given in VI and VII.

$$Re_2(CO)_{10} + H^- \rightarrow [Re_2(CO)_9(CHO)]^- \qquad \Delta H = -263 \text{ kJ/mol} \quad \text{(VI)}$$

$$Fe(CO)_5 + H^- \rightarrow [Fe(CO)_4(CHO)]^- \qquad \Delta H = -260 \text{ kJ/mol} \quad \text{(VII)}$$

The hydride affinity *HA* of $Fe(CO)_5$ is experimentally known, and our value of 260 kJ/mol comes close to the upper range of $HA = 234 \pm 17$ kJ/mol, which Lane and Squires derived from gas-phase hydride transfer reactions.[25] Both metal carbonyls possess a similar hydride affinity around 260 kJ/mol. The heterolytic bond cleavage of **3** in the gas phase, as shown in eq VIII, is determined by charge separation and is highly endothermic.

$$\mathbf{3} \rightarrow [Mo(CO)(NO)(PMe_3)_3]^+ + H^- \qquad \Delta H = 610 \text{ kJ/mol} \quad \text{(VIII)}$$

If we wish to discuss possible reaction mechanisms involving charged species in solution, it is necessary to include solvation effects. A rough estimate for solvation energies can be obtained applying a simple electrostatic continuum model derived by Born and Onsager.[26] The energetics for hydride and hydrogen transfer to $Re_2(CO)_{10}$ and $Fe(CO)_5$ in toluene are compared in eqs XI and X, and XI and XII, respectively.

(24) Lane, K. R.; Sallans, L.; Squires, R. R. *J. Am. Chem. Soc.* **1985**, *107*, 5369.
(25) Lane, K. R.; Squires, R. R. *Polyhedron* **1988**, *7*, 1609.
(26) (a) Born, M. *Z. Phys.* **1920**, *1*, 45. (b) Onsager, L. *J. Am. Chem. Soc.* **1936**, *58*, 1486. (c) Rashin, A. A.; Honig, B. *J. Phys. Chem.* **1985**, *89*, 5588.

$$\mathbf{3} + Re_2(CO)_{10} \rightarrow [Mo(CO)(NO)(PMe_3)_3]^{\bullet} + [Re_2(CO)_9(CHO)]^{\bullet} \quad \Delta H = 233 \text{ kJ/mol} \quad \text{(IX)}$$

$$\mathbf{3} + Re_2(CO)_{10} \rightarrow [Mo(CO)(NO)(PMe_3)_3]^{+} + [Re_2(CO)_9(CHO)]^{-} \quad \Delta H = 210 \text{ kJ/mol} \quad \text{(X)}$$

$$\mathbf{3} + Fe(CO)_5 \rightarrow [Mo(CO)(NO)(PMe_3)_3]^{\bullet} + [Fe(CO)_4(CHO)]^{\bullet} \quad \Delta H = 190 \text{ kJ/mol} \quad \text{(XI)}$$

$$\mathbf{3} + Fe(CO)_5 \rightarrow [Mo(CO)(NO)(PMe_3)_3]^{+} + [Fe(CO)_4(CHO)]^{-} \quad \Delta H = 187 \text{ kJ/mol} \quad \text{(XII)}$$

Hydride transfer processes to $Fe(CO)_5$ are energetically favored over those to $Re_2(CO)_{10}$. This is a solvation effect, since both transition metal carbonyls possess comparable hydride affinities. We further observe that in the case of $Re_2(CO)_{10}$, hydride shift is energetically favored over hydrogen shift, whereas for $Fe(CO)_5$ both processes are accompanied by comparable changes in energy. The radical transfer in turn holds an explanation why the reaction between **3** and $Fe(CO)_5$ is not at equilibrium. The bond formation between $[Mo(CO)(NO)(PMe_3)_3]^{\bullet}$ and $[Fe(CO)_4(CHO)]^{\bullet}$ requires a preparation energy[27] of about 85 kJ/mol, which is needed to distort the iron fragment from its ground-state structure to the geometric arrangement of the final adduct. This process thus kinetically stabilizes the bond between the metal fragments in **7a** and inhibits back reaction.

**X-ray Diffraction Studies on 2, 3, 4b, 7a, 7b, and 8.** The structural features of the $\eta^1$-$BH_4$ complex **2** remain a rarity[28] among the versatile bonding modes found for $BH_4$ units. The examples $FeH(\eta^1\text{-}BH_4)(dmpe)_2$[29] and $FeH(\eta^2\text{-}BH_4)[MeC(CH_2PPh_2)_3]$[30] demonstrate that the ancillary ligand sphere may play a crucial role to determine the coordination mode of the $BH_4$ moiety. Parallel to this and knowing about the structures of the related complexes $W(CO)(NO)(PR_3)_2(\eta^2\text{-}BH_4)$,[31] **2** also seems to be a case for ligand sphere enforced $\eta^1$-binding caused by the phosphine tris-substitution.

A crystal of **2** suitable for an X-ray analysis was obtained from a saturated $Et_2O$ solution by cooling it to −30 °C. The X-ray data collection and processing parameters of **2** are given in Table 1. Figure 3 shows a structural model of **2**.

The asymmetric unit of **2** contains two independent molecules, and in each molecule the Mo center is pseudo-octahedrally coordinated with three $PMe_3$ ligands in meridional position and the $BH_4^-$ unit and the nitrosyl trans to each other. The Mo−N distances are both on the short side of Mo−NO interactions, indicating a strongly bound nitrosyl ligand and concomitantly a strong trans influence exerted by it. Although the obtained $Mo-H_{BH_4}$ distances have to be taken with caution, they seem to be rather long in both molecules (Table 2) and longer than in **3** (see below), allowing one to conclude a weak binding of this group and thus confirming the mentioned strong trans influence of the NO moiety. The $BH_4$ units furthermore display typical hinging with Mo−H−B angles of 142.4° and 128.5°; the wide spread of this angle may indicate a soft energy surface for the bending at the Mo-bound hydrogen, which in turn may be taken as a hint that the $BH_4$ unit is only weakly attached to the metal fragment.

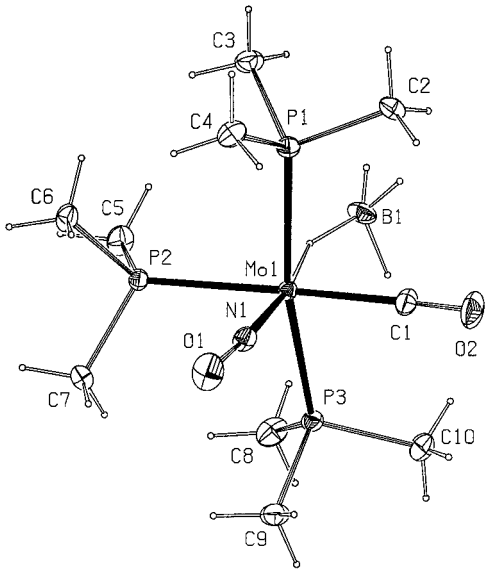


**Figure 3.** ORTEP plot of the structure of **2**. Only the complex of Mo(1) is shown. The thermal ellipsoids are drawn with 20% probability.

Complex **3** showed extraordinary hydride reactivity, which made it interesting to see whether its structure would reveal unusual geometric parameters. Suitable crystals were precipitated from hexane solution by cooling it to −30 °C. The X-ray data collection and processing parameters of **3** are given in Table 1. Figure 4 shows the structural model of one of the two independent molecules of **3** in the unit cell, which both display octahedral coordination of the molybdenum centers. The structures of the $Mo(CO)(NO)(PMe_3)_3$ fragments are similar to those in **2**; however, they differ in the equatorial angles. While in the molecule of Mo(1) both angles of the trans substituents are close to each other (164.88(2)° and 168.6(1)°), in the molecule of Mo(2) they differ significantly (153.83(2)° and 178.3(1)°). The sum of both angles at each Mo center is about the same, indicating an overall "constant" distortion, i.e., the leaning over to the hydride ligand.[3b] It is furthermore noteworthy that the Mo−H bonds are quite long (1.84(3) and 1.83(3) Å)[32] (Table 2). These H atoms were localized in the difference Fourier maps and could be refined. Due to the large diffracting volume of the crystal (Table 1), the reasonable isotropic displacement parameters of the hydrogens (0.064(10) Å$^2$ for H(1) and 0.049(8) Å$^2$ for H(2)) and *R* factors of the structure determination, it is believed that the H positions can be taken with confidence.

The X-ray diffraction study of **4b** was carried out because of its relative uniqueness as an organometallic



(27) Jacobsen, H.; Ziegler, T. *Inorg. Chem.* **1996**, *35*, 775.
(28) (a) Takusagawa, F.; Fumagalli, A.; Koetzle, T. F.; Shore, S. G.; Schmitkons, T.; Fratini, A. V.; Morse, K. W.; Wei, C.-Y.; Bau, R. *J. Am. Chem. Soc.* **1981**, *103*, 5165. (b) Ghilardi, C. A.; Midollini, S.; Orlandini, A. *Inorg. Chem.* **1982**, *21*, 4096. (c) Fryzuk, M. D.; Rettig, S. J.; Westerhaus, A.; Williams, H. D. *Inorg. Chem.* **1985**, *24*, 4316. (d) Jensen, J. A.; Girolami, G. S. *J. Am. Chem. Soc.* **1988**, *110*, 4450. (e) Dionne, M.; Hao, S.; Gambarotta, S. *Can. J. Chem.* **1995**, *73*, 1126.
(29) Bau, R.; Yuan, H. S. H.; Baker, M. V.; Field L. D. *Inorg. Chim. Acta* **1986**, *114*, L27.
(30) Ghilardi, C. A.; Innocenti, P.; Midollini, S.; Orlandini, A. *J. Chem. Soc., Dalton Trans.* **1985**, 605.
(31) Van der Zeijden, A. A. H.; Veghini, D.; Berke, H. *Inorg. Chem.* **1992**, 31, 5106.

**Table 1. Summary of X-ray Diffraction Studies for 2, 3, and 4b**

| | 2 | 3 | 4b |
|---|---|---|---|
| formula | $C_{10}H_{31}BMoNO_2P_3$ | $C_{10}H_{28}MoNO_2P_3$ | $C_{26}H_{41}MoNO_3P_3$ |
| color | orange | orange | yellow |
| cryst dimens (mm) | 0.48 × 0.28 × 0.18 | 0.78 × 0.56 × 0.53 | 0.51× 0.44 × 0.32 |
| cryst syst | monoclinic | orthorhombic | momoclinic |
| space group (No.) | $P2_1/a$ (14) | $P2_12_12_1$ (19) | $P2_1/c$ (14) |
| $a$ (Å) | 15.9680(12) | 14.2303(12) | 15.6439(10) |
| $b$ (Å) | 9.3075(5) | 15.8054(17) | 9.8719(4) |
| $c$ (Å) | 26.911(2) | 16.4491(16) | 19.9105(13) |
| $\beta$ (deg) | 96.916(9) | | 100.877(8) |
| $V$ (Å$^3$) | 3970.4(5) | 3699.7(6) | 3019.6(3) |
| $Z$ | 8 | 8 | 4 |
| fw | 397.02 | 383.18 | 604.45 |
| $d$(calcd) (g cm$^{-3}$) | 1.328 | 1.376 | 1.330 |
| abs coeff (mm$^{-1}$) | 0.898 | 0.962 | 0.619 |
| $F$(000) | 1648 | 1584 | 1260 |
| $2\theta$ scan range (deg) | 5.08 < $2\theta$ < 56.06 | 4.96 < $2\theta$ < 56.08 | 5.52 < $2\theta$ < 60.66 |
| no. of unique data | 9526 | 8731 | 8964 |
| no. of data obsd [$I > 2\sigma(I)$] | 7077 | 7856 | 5950 |
| abs corr | numerical, 14 crystal faces | numerical, 19 cryst. faces | numerical, 17 cryst. faces |
| solution method | Patterson | Patterson | Patterson |
| no. of params refined | 329 | 315 | 308 |
| $R$, wR2 (%) all data | 4.79, 9.98 | 2.75, 5.50 | 5.67, 6.24 |
| R1 (obsd) (%)[a] | 3.38 | 2.28 | 3.23 |
| goodness-of-fit | 0.972 | 1.047 | 1.007 |

[a] $R1 = \sum(F_o - F_c)/\sum F_o$; $I > 2\sigma(I)$; $wR2 = \{\sum w(F_o^2 - F_c^2)^2/\sum w(F_o^2)^2\}^{1/2}$.

**Table 2. Selected Bond Lengths [Å] and Bond Angles [deg] of Both Molecules of 2 and 3**

| 2 | | 3 | |
|---|---|---|---|
| Mo(1)−N(1) | 1.773(3) | Mo(1)−N(1) | 1.811(2) |
| Mo(1)−C(1) | 2.017(4) | Mo(1)−C(1) | 1.988(3) |
| Mo(1)−P(3) | 2.4898(9) | Mo(1)−P(3) | 2.4835(7) |
| Mo(1)−P(1) | 2.4924(9) | Mo(1)−P(1) | 2.4769(7) |
| Mo(1)−P(2) | 2.5159(9) | Mo(1)−P(2) | 2.5172(6) |
| Mo(1)−H(21) | 1.9057(3) | Mo(1)−H(1) | 1.84(3) |
| N(1)−O(1) | 1.204(4) | N(1)−O(2) | 1.204(3) |
| C(1)−O(2) | 1.135(5) | C(1)−O(1) | 1.153(3) |
| Mo(2)−N(2) | 1.781(3) | Mo(2)−N(2) | 1.818(2) |
| Mo(2)−C(11) | 2.002(3) | Mo(2)−C(11) | 1.982(3) |
| Mo(2)−P(6) | 2.487(1) | Mo(2)−P(6) | 2.4686(7) |
| Mo(2)−P(4) | 2.501(1) | Mo(2)−P(4) | 2.4536(6) |
| Mo(2)−P(5) | 2.532(1) | Mo(2)−P(5) | 2.5263(6) |
| Mo(2)−H(26) | 2.0748(3) | Mo(2)−H(2) | 1.83(3) |
| N(2)−O(3) | 1.206(4) | N(2)−O(4) | 1.211(3) |
| O(4)−C(11) | 1.147(4) | O(3)−C(11) | 1.151(3) |
| P(1)−Mo(1)−P(3) | 167.57(3) | P(1)−Mo(1)−P(3) | 164.88(2) |
| P(2)−Mo(1)−C(1) | 178.8(1) | P(2)−Mo(1)−C(1) | 168.6(1) |
| N(1)−Mo(1)−H(21) | 167.2(1) | N(1)−Mo(1)−H(1) | 176(1) |
| P(4)−Mo(2)−P(6) | 164.31(3) | P(4)−Mo(2)−P(6) | 153.83(2) |
| P(5)−Mo(2)−C(11) | 175.5(1) | P(5)−Mo(2)−C(11) | 178.25(8) |
| N(2)−Mo(2)−H(26) | 166.2(1) | N(2)−Mo(2)−H(2) | 178.0(9) |
| Mo(1)−H(26)−B(1) | 142.4 | | |
| Mo(2)−H(26)−B(2) | 128.5 | | |

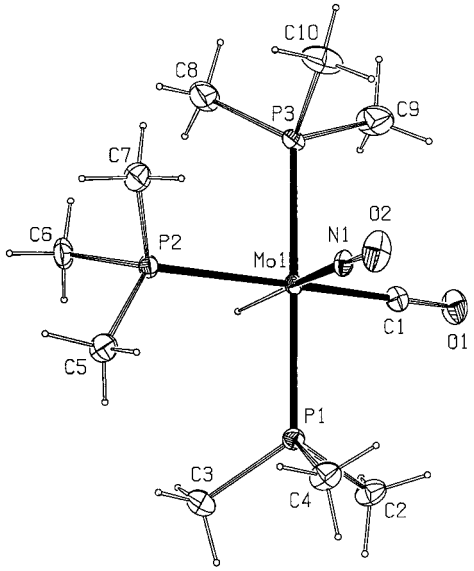


**Figure 4.** ORTEP plot of the structure of **3**. Only the complex of Mo(1) is shown. The thermal ellipsoids are drawn with 20% probability.

alkoxide with a metal center in low oxidation state and the supposed medium strength of the Mo−O bond indicated by the low values of the presumably comparable calculated homolytic BDEs of **7a** and **7b** and those higher values found in the early transition metal, lanthanide, and actinide series.[1b] Such species of middle transition metal elements and terminal alkoxide groups have only rarely been structurally characterized.[33b] Crystals suitable for X-ray analysis were obtained by slow cooling of a saturated hexane/benzene solution (9:1) to −30 °C. Under these conditions **4b** crystallizes as a benzene solvate. The unique phosphorus ligand displayed rotational disorder in the methyl groups, which could be refined by an appropriate occupancy ratio (63/37%). The pseudo-octahedral complex shows a molybdenum environment similar to those of compounds **2**, **3**, and **7** (Figure 5). The Mo−O distance, 2.091(1) Å, is on the long side of the scale for Mo−

(32) Neutron diffraction studies: (a) Schultz, A. J.; Stearley, K. L.; Williams, J. M.; Mink, R.; Stucky G. D. *Inorg. Chem.* **1977**, *16*, 3303. (b) Brammer, L.; Zhao, D.; Bullock, R. M.; McMullan, R. K. *Inorg. Chem.* **1993**, *32*, 4819. X-ray diffraction studies: (c) Petri, S. H. A.; Neumann, B.; Stammler, H. G.; Jutzi, P. *J. Organomet. Chem.* **1998**, *553*, 317. (d) Minato, M.; Sakai, H.; Weng, Z. G.; Zhou, D. Y.; Kurishima, S., Ito, T.; Yamasaki, M.; Shiro, M.; Tanaka, M.; Osakada, K. *Organometallics* **1996**, *15*, 4863. (e) Luo, X. L.; Kubas, G. J.; Burns, C. J. Butcher, R. J. *Organometallics* **1995**, *14*, 3370. (f) Xu, S. S.; Gong, J. F.; Zhou, X. Z. *Chem. J. Chin. Univ.* **1998**, *19*, 70. (g) Thi, N. P. D.; Spichiger, S.; Paglia, P.; Bernardinelli, G.; Kündig, E. P.; Tinns, P. L. *Helv. Chim. Acta* **1992**, *75*, 2593. (h) Dawson, D. M.; Henderson, R. A.; Hills, A.; Hughes, D. L. *J. Chem. Soc., Dalton Trans.* **1992**, 969.

(33) (a) Brandts, J. A. M.; Boersma, J.; Spek, A. L.; van Koten, G. *Eur. J. Inorg. Chem.* **1999**, 1727. (b) McQuillan, F. S.; Chen, H. L.; Hamor, T. A.; Jones, C. J.; Jones, H. A.; Sidebotham, R. P. *Inorg. Chem.* **1999**, 38, 1555. (c) Orpen, A. G.; Brammer, L.; Allen, F. H.; Kennard, O.; Watson, D. G.; Taylor, R. *J. Chem. Soc., Dalton Trans.* **1989**, *S1*, 1.

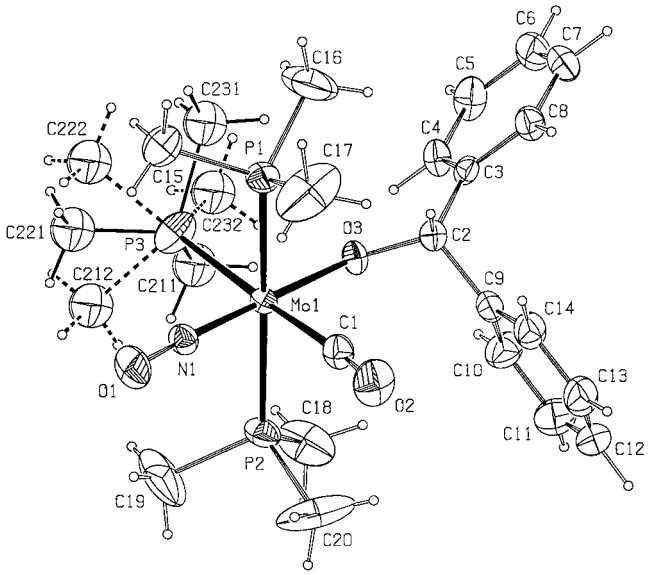


**Figure 5.** ORTEP plot of the structure of **4b**. The thermal ellipsoids are drawn with 50% probability. The benzene solvate molecule is omitted.

**Table 3. Selected Bond Lengths [Å] and Angles [deg] for 4b**

| | |
|---|---|
| Mo(1)−N(1) | 1.796(2) |
| Mo(1)−C(1) | 1.997(2) |
| Mo(1)−O(3) | 2.091(1) |
| Mo(1)−P(2) | 2.4964(6) |
| Mo(1)−P(1) | 2.5024(6) |
| Mo(1)−P(3) | 2.5557(7) |
| N(1)−O(1) | 1.210(2) |
| C(1)−O(2) | 1.144(3) |
| C(2)−O(3) | 1.396(2) |
| N(1)−Mo(1)−C(1) | 85.72(8) |
| N(1)−Mo(1)−O(3) | 177.59(7) |
| C(1)−Mo(1)−O(3) | 96.08(7) |
| N(1)−Mo(1)−P(2) | 87.91(6) |
| O(3)−Mo(1)−P(2) | 90.55(4) |
| N(1)−Mo(1)−P(1) | 87.59(6) |
| P(2)−Mo(1)−P(1) | 174.36(2) |
| N(1)−Mo(1)−P(3) | 97.12(6) |
| P(2)−Mo(1)−P(3) | 92.92(2) |
| P(1)−Mo(1)−P(3) | 91.00(2) |

$O_{alkoxide}$ interactions[33] (Table 3, compare also structures of **7** and **8**). This effect appears to be caused by a strong trans influence of the NO group,[34] which is mainly a $\sigma$-bonding effect. Concomitantly $\pi$ donation in the Mo−O bond is also reduced. It should be mentioned that in specific cases the $\sigma$-type trans influence of the NO group may be overcompensated by $\pi$ push−pull effects, which may lead to unexpectedly short M−($\pi$ donor) distances.[34a−c] The Mo−O−$CHPh_2$ angle of **4b** is rather wide, 126.2(1)°. For the most part we attribute this to the steric bulk of the benzhydryl residue.

The structures of **7a** and **7b** were also determined by X-ray diffraction studies. Suitable crystals of both complexes were obtained by slow cooling of saturated ether solutions to −30 °C. Their structures are displayed in Figure 6a,b. The crystallographic and refinement

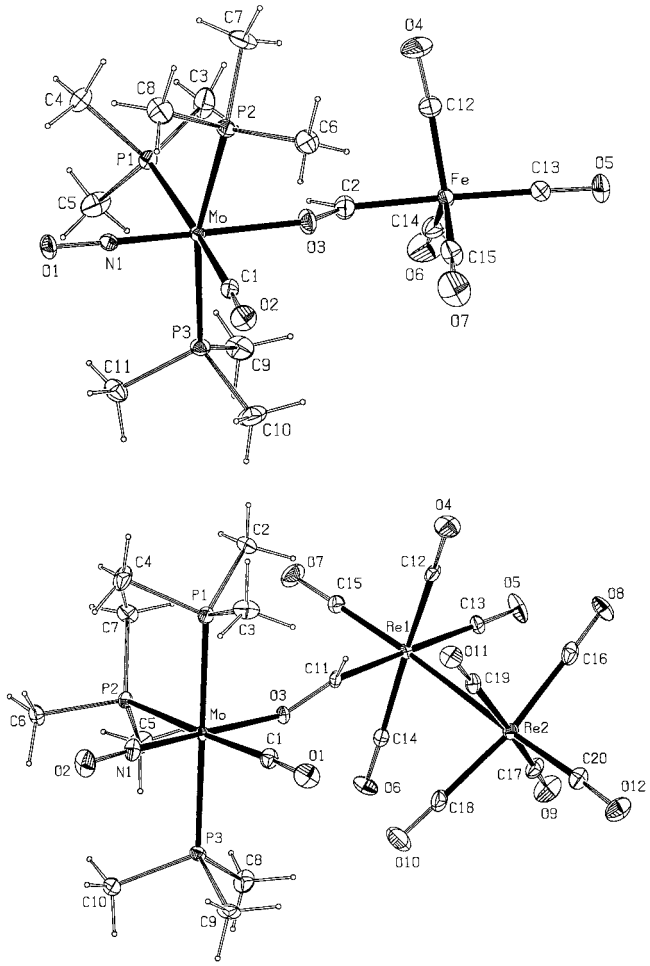


**Figure 6.** ORTEP plots of the structures of **7a** (above) and **7b** (below). The ellipsoids are drawn with 20% probability.

data are listed in Table 4. Selected bond lengths and angles are given in Table 5. As mentioned before, insertion of a metal carbonyl unit into a M−H bond has rarely been seen in transition metal hydride chemistry. Consequently, since this represents the major synthetic access to $\mu$-formyl complexes, such species have only rarely been subjected to X-ray crystallographic studies.[18g,35]

The coordination geometries around the Mo centers show great similarities with only slight deviations from an ideal octahedral arrangement (Table 5 and Figure 6). Only for **7a** does one find a more pronounced bending of the trans-arranged phosphorus ligands toward the formyl moiety. The iron center of **7a** is pseudo-trigonal bipyramidally coordinated like in the parent $[Fe(CO)_4CHO]^-$ anion.[19] Also the structure of the $Re_2(CO)_9CHO$ unit of **7b** is stereochemically related to that of $[Re_2(CO)_9CHO]^-$,[20] bearing the formyl groups in equatorial positions. The angles of the $\mu^2$-formyl group at the $C_{formyl}$ atom are very similar and both significantly larger than 120°, which is typical of transition metal $\mu^2$-acyl arrangements.[18g,34,35] The $\mu$-formyl C−O distances of **7a** and **7b** are noticably different, with a longer separation of the rhenium complex **7b** indicating a stronger $\pi$−donating capacity of the $Re_2(CO)_9$

(34) (a) Veghini, D.; Nefedov, S. E.; Schmalle, H.; Berke, H. *J. Organomet. Chem.* **1996**, *526*, 117. (b) Veghini, D.; Berke, H. *Inorg. Chem.* **1996**, *35*, 4770. (c) Lyne, P. D.; Mingos, D. M. P. *J. Chem. Soc., Dalton Trans.* **1995**, 1635. (d) Huheey, J. E.; Keiter, E. A.; Keiter, R. L. *Inorganic Chemistry*, 4th ed.; Harper Collins College Publisher: New York, 1993. (e) Richter-Addo, G. B.; Legzdins, P. *Metal Nitrosyls*; Oxford University Press: New York, 1992.

(35) (a) Wolczanski, P. T.; Threlkel, R. S.; Santarsiero, B. D. *Acta Crystallogr. Sect. C* **1983**, *39*, 1330. (b) Barger, P. T.; Santarsiero, B. D.; Armantrout, J.; Bercaw, J. E. *J. Am. Chem. Soc.* **1984**, *106*, 5178.

**Table 4. Summary of X-ray Diffraction Studies 7a, 7b, and 8**

| | 7a | 7b | 8 |
|---|---|---|---|
| formula | $C_{15}H_{28}FeMoNO_7P_3$ | $C_{20}H_{28}MoNO_{12}P_3Re_2$ | $C_{13}H_{28}MoN_2O_4P_2$ |
| color | yellow | yellow-orange | red |
| cryst dimens (mm) | 0.49 × 0.48 × 0.27 | 0.41 × 0.18 × 0.16 | 0.66 × 0.64 × 0.23 |
| cryst syst | orthorhombic | monoclinic | orthorhombic |
| space group (No.) | *Pbca* (61) | $P2_1/n$ (14) | $P2_12_12_1$ (19) |
| *a* (Å) | 12.6177(6) | 9.6511(9) | 10.7371(7) |
| *b* (Å) | 13.6232(9) | 26.513((3) | 16.1098(13) |
| *c* (Å) | 29.1957(16) | 13.2522(12) | 23.2055(15) |
| $\beta$ (deg) | | 99.96(1) | |
| *V* (Å$^3$) | 5018.6(5) | 3339.8(6) | 4013.9(5) |
| *Z* | 8 | 4 | 8 |
| fw | 579.08 | 1035.68 | 434.25 |
| *d*(calcd) (g cm$^{-3}$) | 1.533 | 2.060 | 1.437 |
| abs coeff (mm$^{-1}$) | 1.300 | 7.795 | 0.828 |
| *F*(000) | 2352 | 1952 | 1792 |
| 2$\theta$ scan range (deg) | 4.26 < 2$\theta$ < 53.52 | 4.56 < 2$\theta$ < 51.76 | 5.84 < 2$\theta$ < 60.68 |
| no. of unique data | 5287 | 6130 | 11 792 |
| no. of data obsd [$I > 2\sigma(I)$] | 4067 | 4571 | 9114 |
| abs corr | numerical, 16 cryst faces | numerical, 11 cryst faces | numerical, 12 cryst faces |
| solution method | Patterson | Patterson | Patterson |
| no. of params refined | 257 | 356 | 397 |
| *R*, wR2 (%) all data | 3.72, 6.45 | 3.69, 6.58 | 4.25, 5.61 |
| R1, (obsd) (%)[a] | 2.77 | 2.49 | 2.95 |
| goodness-of-fit | 1.107 | 1.050 | 1.014 |

[a] $R1 = \sum(F_o - F_c)/\sum F_o$; $I > 2\sigma(I)$; $wR2 = \{\sum w(F_o^2 - F_c^2)^2/\sum w(F_o^2)^2\}^{1/2}$.

**Table 5. Selected Bond Lengths [Å] and Bond Angles [deg] of 7a and 7b**

| 7a | | 7b | |
|---|---|---|---|
| Mo−P(2) | 2.5028(7) | Mo−P(3) | 2.498(2) |
| Mo−O(3) | 2.173(2) | Mo−O(3) | 2.173(5) |
| Mo−P(3) | 2.5102(7) | Mo−P(1) | 2.528(2) |
| Mo−C(1) | 2.015(3) | Mo−C(1) | 1.970(7) |
| Mo−N(1) | 1.774(2) | Mo−N(1) | 1.772(6) |
| Mo−P(1) | 2.5444(7) | Mo−P(2) | 2.556(2) |
| N(1)−O(1) | 1.210(3) | N(1)−O(2) | 1.204(8) |
| C(1)−O(2) | 1.136(3) | C(1)−O(1) | 1.172(9) |
| C(2)−O(3) | 1.188(4) | C(11)−O(3) | 1.265(8) |
| Fe−C(2) | 1.917(3) | Re(1)−C(11) | 2.102(7) |
| N(1)−Mo−O(3) | 178.56(8) | N(1)−Mo−O(3) | 176.4(2) |
| P(2)−Mo−P(3) | 166.06(2) | P(3)−Mo−P(1) | 175.91(7) |
| C(1)−Mo−P(1) | 174.54(8) | C(1)−Mo−P(2) | 173.9(2) |
| C(2)−O(3)−Mo | 143.3(2) | C(11)−O(3)−Mo | 127.8(5) |
| O(3)−C(2)−Fe | 130.7(3) | O(3)−C(11)−Re(1) | 127.5(5) |

fragment. Both $\mu$-(C−O) bond lengths fall into the expected range of transition metal bridged acyl compounds.[35,36] However, due to their relative shortness, they do not match with an oxycarbene structure.[18g,35]

To support the spectroscopically derived structure of **8**, an X-ray crystal structure determination was carried out. Suitable crystals of **8** were grown from pentane by slow cooling of a solution to −30 °C. The crystallographic and refinement data are listed in Table 4. The structure of **8** is displayed in Figure 7 showing only one independent molecule of the unit cell. **8** crystallizes in the chiral space group $P2_12_12_1$. Thus, the structure determination

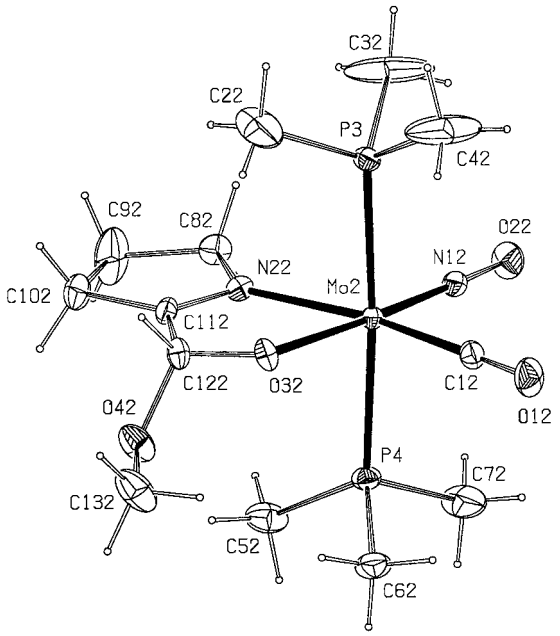


**Figure 7.** ORTEP plot of the structure of **8**. Only the complex of Mo(2) is shown. Thermal ellipsoids are drawn with 20% probability.

was carried out on an enantiomerically pure crystal of **8** with opposite configuration on C121 and C122 of the independent molecules. As a consequence of the absence of a crystallographic mirror plane, both molecules of **8** cannot be mirror images and therefore should deviate in bonding parameters as given in Table 6 and display different conformations. The Mo centers of both molecules are pseudo-octahedral with a practically planar N,O-chelate ring, two almost trans-disposed $PMe_3$ groups, and the CO and the NO ligands in cis position. There is no significant difference in the Mo−P bond lengths (see Table 4). Finally it should be emphasized that the Mo−O distances of both molecules of **8** are similar to those of **4b** and correspond to elongated values. As for **4b**, this is thought to be due to the NO trans influence.

(36) Selected references: Jensen, C. M.; Knobler, C. B.; Kaesz, H. D. *J. Am. Chem. Soc.* **1984**, *106*, 5926. Sünkel, K.; Nagel, U.; Beck, W. *J. Organomet. Chem.* **1983**, *251*, 227. Jeffery, J. C.; Orpen, A. G.; Stone, F. G. A.; Went, M. J. *J. Chem. Soc., Dalton Trans.* **1986**, 173. Kampe, C. E.; Broag, N. M.; Kaesz, H. D. *J. Mol. Catal.* **1983**, *21*, 297. Kreiter, C. G.; Franzreb, K.-H.; Sheldrick, W. S. *J. Organomet. Chem.* **1984**, *270*, 71. Lenhert, P. G.; Lukehart, C. M.; Warfield, L. T. *Inorg. Chem.* **1980**, *19*, 311. Lugan, N.; Lavigne G.; Bonnet J.-J. *Inorg. Chem.* **1987**, *26*, 585. Bonnesen, P. V.; Baker, A. T.; Hersh, W. H. *J. Am. Chem. Soc.* **1986**, *108*, 8304. Chen, Y.-J.; Knobler, C. B.; Kaesz, H. D. *Polyhedron* **1988**, *7*, 1891. Longato, B.; Norton, J. R.; Huffmann, J. C.; Marsella, J. A.; Caulton, K. G. *J. Am. Chem. Soc.* **1981**, *103*, 209. Lippmann, E.; Robl, C.; Berke, H.; Kaesz, H. D.; Beck, W. *Chem. Ber.* **1993**, *126*, 933. Xu, D. Q.; Kaesz, H. D.; Khan, S. I. *Inorg. Chem.* **1991**, *30*, 1341.

**Table 6. Selected Bond Lengths [Å] and Bond Angles [deg] of Both Molecules of 8**

| | | | |
|---|---|---|---|
| Mo(1)−N(11) | 1.791(2) | Mo(2)−N(12) | 1.797(2) |
| Mo(1)−C(11) | 1.956(3) | Mo(2)−C(12) | 1.971(3) |
| Mo(1)−O(31) | 2.099(2) | Mo(2)−O(32) | 2.117(2) |
| Mo(1)−N(21) | 2.209(2) | Mo(2)−N(22) | 2.209(2) |
| Mo(1)−P(2) | 2.4870(9) | Mo(2)−P(4) | 2.4891(8) |
| Mo(1)−P(1) | 2.5049(9) | Mo(2)−P(3) | 2.4910(3) |
| C(11)−O(11) | 1.162(4) | C(12)−O(12) | 1.153(4) |
| N(11)−O(21) | 1.209(3) | N(12)−O(22) | 1.209(3) |
| N(21)−C(111) | 1.280(4) | N(22)−C(112) | 1.276(4) |
| O(31)−C(121) | 1.360(4) | O(32)−C(122) | 1.328(3) |
| N(11)−Mo(1)−C(11) | 89.6(1) | N(12)−Mo(2)−C(12) | 91.4(1) |
| C(11)−Mo(1)−O(31) | 96.3(1) | C(12)−Mo(2)−O(32) | 93.1(1) |
| N(11)−Mo(1)−N(21) | 99.7(1) | N(12)−Mo(2)−N(22) | 101.4(1) |
| O(31)−Mo(1)−N(21) | 74.42(9) | O(2)−Mo(2)−N(22) | 74.12(8) |
| P(2)−Mo(1)−P(1) | 176.06(3) | P(4)−Mo(2)−P(3) | 175.88(3) |

## Conclusions

Our investigations of the $Mo(CO)(H)(NO)(PMe_3)_3$ complex (**3**) revealed an exceptionally high reactivity of the Mo−H bond. The found high propensity for carbonyl insertion resembles closely that of metallocene hydride compounds with early transition metal centers.[37] To a major degree we attribute this to the influence of the coordinative environment of this compound, specifically to the effect of the nitrosyl group.[2,34] The nitrosyl group "tunes" the metal center toward lower electronegativity and furthermore exerts a strong trans influence. H ligands activated by at least one of these effects should display lower covalency of the $L_nM-H$ bond. As a consequence, enhanced hydridicity[4e] and a strong potential for hydride transfer reactions as for **3** and other complexes[38] results.

## Experimental Part

All reactions and manipulations were performed under a dry $N_2$ atmosphere by conventional Schlenk techniques or in a glovebox. Solvents were dried by standard methods and freshly distilled before use. NMR spectra: Varian Gemini-300 instrument; $^1H$ at 300.08 MHz, $^{13}C$ at 75.46 MHz, $^{31}P$ at 121.47 MHz, $^{11}B$ at 96.2 MHz. $\delta$ ($^1H$), $\delta$ ($^{13}C$) rel to $SiMe_4$ and $\delta$ ($^{31}P$) rel to $H_3PO_4$, and $\delta$($^{11}B$) rel to $BF_3{\cdot}OEt_2$. IR spectra: Biorad FTS-45 instrument. Raman spectra: Renishaw Labram Raman microscope. Mass spectra: Finnigan-MAT-8400 spectrometer; FAB spectra in 3-nitrobenzyl alcohol matrix.

**Preparation of *mer*-Mo(Cl)(CO)(NO)($PMe_3$)$_3$ (1).** To a stirred solution of 4.50 g (11.1 mmol) of *trans*-$Mo(CO)_4(NO)(ClAlCl_3)$ in 200 mL of THF, prepared according to a literature procedure,[8] was syringed 5.0 mL (48.5 mmol) of $PMe_3$. The mixture was vacuum transferred into an autoclave and then heated to 80 °C. After 48 h (IR monitoring) the mixture was cooled to room temperature and then cannula transferred into a frit. After filtration the filtrate was dried in vacuo and the remaining residue was extracted with $Et_2O$. Removal of $Et_2O$ in vacuo afforded a yellow solid. Yield: 3.30 g (71%). IR ($cm^{-1}$ THF): 1931 (CO), 1597 (NO). $^1H$ NMR ($C_6D_6$): 1.25 (t, $^2J_{HP}$ = 3.2 Hz, 18H, 2$PMe_3$ trans); 1.06 (d, $^2J_{HP}$ = 6.4 Hz, 9H, $PMe_3$). $^{13}C\{^1H\}$ NMR($C_6D_6$): 230.0 (dt, $^2J_{CPcis}$ = 10 Hz, $^2J_{Cptrans}$ = 56 Hz, CO); 17.0 (dt, $^1J_{CP}$ = 19 Hz, $^3J_{CP}$ = 3 Hz, $PMe_3$, 17.6 (td, $^1J_{CP}$ = 11 Hz, $^3J_{CP}$ = 1 Hz, 2$PMe_3$ trans). $^{31}P\{^1H\}$ NMR ($C_6D_6$): −10.3 (d, $^2J_{PP}$ = 30 Hz, 2$PMe_3$ trans), −17.5 (t, $^2J_{PP}$ = 30 Hz, $PMe_3$). EI-MS: 418 (7, $M^+$), 390(78, [$M^+$ − CO]), 388 (63, [$M^+$ − NO]), 360 (8, [$M^+$ − CO − NO]), 314 (100, [$M^+$ − CO − $PMe_3$]), 312(80, [$M^+$ − NO − $PMe_3$]), 283 (37, [$M^+$ − CO − NO − $PMe_3$]), 238 (61, [$M^+$ − CO − 2$PMe_3$]). Anal. Calcd for $C_{10}H_{27}ClMoNO_2P_3$: C 28.75, H 6.53, N 3.35. Found: C 28.88, H 6.28, N 3.37.

**Preparation of *mer*-Mo($HBH_3$)(CO)(NO)($PMe_3$)$_3$ (2).** A 0.55 g (1.32 mmol) sample of **1** and 0.15 g (6.88 mmol) of $LiBH_4$ were placed in a Schlenk tube, then 20 mL of $Et_2O$ was added via a cannula into the solids at −78 °C, and 0.75 mL (7.28 mmol) of $PMe_3$ was introduced via a syringe. The cold bath was removed and the reaction mixture was stirred at room temperature. During this time the yellow suspension changed to an orange, homogeneous solution. After 2 h (IR monitoring) the solution was filtered over Celite and the filtrate was dried in vacuo. The residue was extracted with toluene. Removal of the toluene in vacuo and recrystallization from $Et_2O$ at −30 °C gave orange **2**. Yield: 0.39 g (75%). IR ($cm^{-1}$, THF): 1938 (CO), 1610 (NO). $^1H$ NMR ($C_7D_8$, rt): 1.19 (t, $^2J_{HP}$ = 3.2 Hz, 18H, 2$PMe_3$ trans); 1.03 (br, s, 9H, PMe3), −1.51(br, quart. $^1J_{HB}$ = 86.2 Hz, Mo−*HB*). $^{31}P\{^1H\}$ NMR ($C_7D_8$, rt): −10.3 (s, 2$PMe_3$ trans), −17.4 (br, s, $PMe_3$). $^{11}B$ NMR ($C_7D_8$, rt): −38.5 (quint., $^1J_{BH}$ = 85 Hz). $^1H$ NMR ($C_7D_8$, −40 °C): 1.15 (t, $^2J_{HP}$ = 3.3 Hz, 18H, 2$PMe_3$ trans); 0.93 (d, $^2J_{HP}$ = 6.75 Hz, 9H, $PMe_3$), −1.42 (br, 1H, Mo−*HB*), 1.20 (br, 3H, *BH*$_3$). $^{13}C\{^1H\}$ NMR ($C_7D_8$, −40 °C): 231(dt, $^2J_{CPcis}$ = 10 Hz, $^2J_{CPtrans}$ = 49 Hz, CO); 17.6 (dt, $^1J_{CP}$ = 12 Hz, $^3J_{CP}$ = 2 Hz, $PMe_3$), 18.0 (td, $^1J_{CP}$ = 12 Hz, $^3J_{CP}$ = 1 Hz, $PMe_3$ trans). $^{31}P\{^1H\}$ NMR ($C_7D_8$, −40 °C): −10 (d, $^2J_{PP}$ = 28 Hz, 2 $PMe_3$ trans), −16 (t, $^2J_{PP}$ = 28.1 Hz, $PMe_3$). FAB-MS: 397 (24, $M^+$), 369 (20, [$M^+$ − CO]), 367 (8, [$M^+$ − NO]), 384 (26, [$M^+$ − $BH_3$]), 321 (21, [$M^+$ − $PMe_3$]), 293 (37, [$M^+$ − CO − $PMe_3$]), 217 (32, [$M^+$ − CO − 2$PMe_3$]). Anal. Calcd for $C_{10}H_{31}BMoNO_2P_3$: C 30.25, H 7.89, N 3.53. Found: C 30.61, H 7.42, N 3.66.

**Preparation of *mer*-Mo(CO)(H)(NO)($PMe_3$)$_3$ (3).** To a solution of 0.30 g (0.76 mmol) of **2** in 20 mL of toluene placed in a Schlenk tube was added via syringe 1.20 mL (11.60 mmol) of $PMe_3$. The mixture was stirred at room temperature for 48 h. After this time the solvent was removed in vacuo. The remaining residue was extracted with pentane. Concentration and chilling of the combined solutions to −30 °C gave reddish crystals of **3**. Yield: 0.17 g (58.7%). IR ($cm^{-1}$, hexane, −70 °C): 1916, 1900 (CO), 1609 (MoH), 1596 (NO). IR ($cm^{-1}$, hexane rt): 1918 (CO), 1611 (MoH, NO). Raman ($cm^{-1}$, solid state): 1883 (CO), 1601 (NO, MoH). $^1H$ NMR ($C_6D_6$): 1.27 (t, $^2J_{HP}$ = 3.1 Hz, 18H, 2$PMe_3$ trans); 1.11 (d, $^2J_{HP}$ = 6.2 Hz, 9H, $PMe_3$); −1.92 (dt, $^2J_{HPtrans}$ = 27.8 Hz, $^2J_{HP}$ = 32.5 Hz, 1H, Mo−H). $^{13}C\{^1H\}$ NMR ($C_6D_6$): 239.6 (dt, $^2J_{CPcis}$ = 11 Hz, $^2J_{Cptrans}$ = 37 Hz, CO); 21 (dt, $^1J_{CP}$ = 19 Hz, $^3J_{CP}$ = 3 Hz, $PMe_3$), 21.9 (td, $^1J_{CP}$ = 12 Hz, $^3J_{CP}$ = 2 Hz, 2$PMe_3$ trans). $^{31}P\{^1H\}$ NMR ($C_6D_6$): −4.1 (d, $^2J_{PP}$ = 29 Hz, 2$PMe_3$ trans), −11.8 (t, $^2J_{PP}$ = 29 Hz, $PMe_3$). EI-MS: 383 (35, $M^+$), 355 (84, [$M^+$ − CO]), 353 (78, [$M^+$ − NO]), 325 (20, [$M^+$ − CO − NO]), 279 (86, [$M^+$ − CO − $PMe_3$]), 277 (78, [$M^+$ − NO − $PMe_3$]), 248 (24, $M^+$ − CO − NO − $PMe_3$]), 203 (33, [$M^+$ − CO − 2$PMe_3$]). Anal. Calcd for $C_{10}H_{28}MoNO_2P_3$: C 31.34, H 7.38, N 3.66. Found: C 31.00, H 7.63, N 3.67.

**Preparation of *mer*-Mo($OCH_2Ph$)(CO)(NO)($PMe_3$)$_3$ (4a).** A 0.0350 g (0.09 mmol) sample of **3** was dissolved in 1 mL of toluene, and benzaldehyde (9.5 $\mu$L, 0.094 mmol) was added. After a few minutes (NMR monitoring) the solvent was removed in vacuo and the residue was extracted with pentane. Concentration and cooling of the combined solutions to −30 °C afforded yellow crystals of **4a**. Yield: 0.039 g (87%). IR ($cm^{-1}$, hexane): 1922 (CO), 1588 (NO). $^1H$ NMR ($C_6D_6$): 7.40 (d, $^3J_{HH}$ = 7.3 Hz, 2H, Ph), 7.28 (t, $^3J_{HH}$ = 7.3 Hz, 2H, Ph), 7.11 (t, $^3J_{HH}$ = 7.3 Hz, 1H, Ph), 4.91 (s, 2H, $CH_2O$), 1.19 (t, $^2J_{HP}$ = 3.0 Hz, 18H, 2$PMe_3$ trans); 1.07 (d, $^2J_{HP}$ = 6.1 Hz, 9H, $PMe_3$). $^{13}C\{^1H\}$ NMR ($C_6D_6$): 231.6 (dt, $^2J_{CPcis}$ = 11 Hz, $^2J_{CPtrans}$ = 56 Hz, CO); 150.0, 127.9, 126.0, 125.6 (4s, Ph), 75.5 (dt, $^3J_{CPtrans}$ = 7.3 Hz, $^3J_{CPtrans}$ = 1 Hz, $CH_2O$), 17.0 (dt, $^1J_{CP}$ = 17 Hz, $^3J_{CP}$ = 3 Hz, $PMe_3$), 17.8 (td, $^1J_{CP}$ = 10 Hz, $^3J_{CP}$ = 1 Hz, 2$PMe_3$ trans). $^{31}P\{^1H\}$ NMR ($C_6D_6$): −9.9 (d, $^2J_{PP}$ = 28 Hz,

(37) Erker, G. *Acc. Chem. Res.* **1984**, *17*, 103.

(38) (a) Rybtchinski, B.; Ben David, Y.; Milstein, D. *Organometallics* **1997**, *16*, 3786. (b) Labinger, J. A. In *Tranistion Metal Hydrides*; Dedieu, A., Ed.; VCH Publishers Inc.: New York, 1992; p 361.

2$PMe_3$ trans), −16.3 (t, $^2J_{PP}$ = 28 Hz, $PMe_3$). FAB-MS: 489 (7, $M^+$), 461 (16, [$M^+$ − CO]), 459 (10, [$M^+$ − NO]), 383 (100, [$M^+$ − PhCHO]), 353 (34, [$M^+$ − CO − $PhCH_2O$]), 307 (18, [$M^+$ − PhCHO − $PMe_3$]), 278 (44, [$M^+$ − CO − $PhCH_2O$ − $PMe_3$]). Anal. Calcd for $C_{17}H_{34}MoNO_3P_3$: C 41.72, H 7.02, N 2.86. Found: C 42.14, H 6.89, N 2.79.

**Preparation of *mer*-Mo(OCHPh$_2$)(CO)(NO)(PMe$_3$)$_3$ (4b).** A mixture of 0.040 g (0.1 mmol) of **3** and 0.019 g (0.1 mmol) of benzophenone in 3 mL of toluene was stirred for 3 h at rt (NMR monitoring). After this time the solvent was evaporated in vacuo. The residue was extracted with pentane, and the combined solutions were concentrated and cooled to −30 °C to afford yellow **4b**. Yield: 0.0480 g (81.4%). IR ($cm^{-1}$, hexane): 1922 (CO), 1588 (NO). $^1$H NMR ($C_6D_6$): 7.44 (d, $^3J_{HH}$ = 7.8 Hz, 2H, Ph), 7.16 (t, $^3J_{HH}$ = 7.8 Hz, 2H, Ph), 7.01 (t, $^3J_{HH}$ = 7.8 Hz, 1H, Ph), 5.55 (s, 1H, OC*H*), 1.06 (t, $^1J_{HP}$ = 2.8 Hz, 18H, $PMe_3$ trans), 1.11 (d, $^2J_{HP}$ = 6.0 Hz, 9H, $PMe_3$). $^{13}$C{$^1$H} NMR ($C_6D_6$): 230.9 (dt, $^2J_{CPcis}$ = 10 Hz, $^2J_{CPtrans}$ = 56.7 Hz, CO); 152.4, 127.9, 127.1, 125.9 (4s, Ph), 87.4 (dt, $^3J_{CP}$ = 6 Hz, $^3J_{CPtrans}$ = 2 Hz, OC*H*),17.3 (dt, $^1J_{CP}$ = 16 Hz, $^3J_{CP}$ = 3 Hz, $PMe_3$), 18.0 (td, $^1J_{CP}$ = 10.0 Hz, $^3J_{CP}$ = 1.2 Hz, 2$PMe_3$trans). $^{31}$P{$^1$H} NMR ($C_6D_6$): −12.9 (d, $^2J_{PP}$ = 29 Hz, 2$PMe_3$ trans), −17.0 (t, $^2J_{PP}$ = 29 Hz, $PMe_3$). FAB-MS: 565 (11, $M^+$), 535 (12, [$M^+$ − NO]), 507 (11, [$M^+$ − CO − NO]), 383 (84, [$M^+$ − $Ph_2CO$]), 354 (48, [$M^+$ − CO − $Ph_2CHO$]), 278 (54, [$M^+$ − CO − $Ph_2CHO$ − $PMe_3$]). Anal. Calcd for $C_{23}H_{38}MoNO_3P_3$: C 48.85, H 6.79, N 2.48. Found: C 48.82, H 6.99, N 2.47.

**Preparation of *mer*-Mo[(OCH(CH$_3$)(Ph)](CO)(NO)(PMe$_3$)$_3$ (4c).** A 0.0350 g (0.09 mmol) sample of **3** was dissolved in 1 mL of toluene, and 12.0 $\mu$L (0.1 mmol) of acetophenone was added. After 7 h (NMR monitoring) the solvent was removed in vacuo and the residue was extracted with pentane. Concentration and cooling to −30 °C of the extracts produced yellow crystals of **4c**. Yield: 0.0420 g (91.3%). IR ($cm^{-1}$, hexane): 1922 (CO), 1584 (NO). $^1$H NMR ($C_6D_6$): 7.36 (d, $^3J_{HH}$ = 7.4 Hz, 2H, Ph), 7.25 (t, $^3J_{HH}$ = 7.4 Hz, 2H,Ph), 7.09 (t, $^3J_{HH}$ = 7.8 Hz, 1H, Ph), 4.62 (quartet, $^3J_{HH}$ = 6.0 Hz, 1H, OC*H*), 1.35 (d, $^3J_{HH}$ = 6.5 Hz, 3H, Me), 1.28 (t, $^2J_{HP}$ = 2.9 Hz, 9H, $PMe_3$ trans); 1.11 (t, $^2J_{HP}$= 2.9 Hz, 9H, $PMe_3$ trans); 1.03 (d, $^2J_{HP}$ = 5.9 Hz, 9H, $PMe_3$). $^{13}$C{$^1$H} NMR ($C_6D_6$): 231.4 (dt, $^2J_{CPcis}$ = 11 Hz, $^2J_{CPtrans}$ = 57 Hz, CO); 154.1, 127.8, 126.1, 128.5 (4s, Ph), 79.1 (dt, $^3J_{CP}$ = 5 Hz, $^3J_{CPtrans}$ = 2 Hz, *OCH*), 30.5 (s, Me), 17.1 (dt, $^1J_{CP}$ = 16 Hz, $^3J_{CP}$ = 3 Hz, $PMe_3$), 18.2 (td, $^1J_{CP}$ = 10 Hz, $^3J_{CP}$ = 1 Hz, $PMe_3$ trans), 18.1 (td, $^1J_{CP}$ = 10 Hz, $^3J_{CP}$ = 1 Hz, $PMe_3$ trans). $^{31}$P{$^1$H} NMR ($C_6D_6$): −12.3 (d, $^2J_{PP}$ = 29 Hz, 2$PMe_3$ trans), −17.5 (t, $^2J_{PP}$ = 29 Hz, $PMe_3$). EI-MS: 503 (12, $M^+$), 475 (100, [$M^+$ − CO]), 473 (58, [$M^+$ − NO]), 427 (60, [$M^+$ − $PMe_3$]), 399 (58, [$M^+$ − CO − $PMe_3$]), 355 (14, [$M^+$ − CO − $PhCOCH_3$]), 323 (55, [$M^+$ − CO − NO − $PhCH_3CHO$]). Anal. Calcd for $C_{18}H_{36}MoNO_3P_3$: C 42.95, H 7.27, N 2.78. Found: C 43.24, H 7.28, N 2.79.

**Preparation of *mer*-Mo[(OCH(CH$_3$)$_2$](CO)(NO)(PMe$_3$)$_3$ (4d).** A 21.0 $\mu$L (0.29 mmol) sample of acetone was added to a solution of 0.055 g (0.14 mmol) of **3** in 5 mL of toluene. The mixture was stirred at rt for 10 h (NMR monitoring). After this time the solvent was removed in vacuo. The residue was extracted with pentane, and the combined solutions were concentrated and cooled to −30 °C to afford yellow **4d**. Yield: 0.0540 g (85.3%). IR ($cm^{-1}$, hexane): 1922 (CO), 1580 (NO). $^1$H NMR ($C_6D_6$): 3.75 (hept, $^3J_{HH}$ = 6 Hz, 1H, OCH), 1.26 (t, $^2J_{HP}$ = 2.9 Hz, 18H, 2$PMe_3$ trans), 1.03 (d, $^2J_{HP}$ = 5.8 Hz, 9H, $PMe_3$), 1.11 (d, $^3J_{HH}$ = 5.8 Hz, 6H, 2$Me_3$). $^{13}$C{$^1$H} NMR ($C_6D_6$): 232.0 (dt, $^2J_{CPcis}$ = 11 Hz, $^2J_{CPtrans}$ = 59 Hz, CO), 70.7 (pseudo-quint, $^3J_{CPtrans}$ = 5 Hz, $^3J_{CPtrans}$ = 2 Hz, OCH), 16.8 (dt, $^1J_{CP}$ = 16 Hz, $^3J_{CP}$ = 3 Hz, $PMe_3$), 18.1 (td, $^1J_{CP}$ = 10 Hz, $^3J_{CP}$ = 1 Hz, 2$PMe_3$ trans). $^{31}$P{$^1$H} NMR ($C_6D_6$): −11.8 (d, $^2J_{PP}$ = 29 Hz, 2$PMe_3$ trans), −18.0 (t, $^2J_{PP}$ = 29 Hz, $PMe_3$). EI-MS: 441 (10, $M^+$), 413 (63, [$M^+$ − CO]), 355 (20, [$M^+$ − CO − $Me_2CO$], 337 (100, [$M^+$ − CO − $PMe_3$]), 335 (100, [$M^+$ − NO − $PMe_3$]), 324 (66, [$M^+$ − CO − NO − $Me_3CO$]). Anal. Calcd for $C_{13}H_{34}MoNO_3P_3$: C 35.38, H 7.78, N 3.17. Found: C 35.02, H 8.23, N 3.17.

**Preparation of *mer*-Mo(OCHO)(CO)(NO)(PMe$_3$)$_3$ (5).** A solution of 0.060 g (0.16 mmol) of **3** in 5 mL of toluene was stirred at rt under 1 bar $CO_2$ for 1 h. After this time the solvent was evaporated in vacuo and the residue was extracted with pentane. Concentration and cooling of the combined solutions to −30 °C afforded yellow crystals of **5**. Yield: 0.057 (85%). IR ($cm^{-1}$, hexane): 1958, 1931 (CO), 1625 (OCO), 1609 (NO). $^1$H NMR ($C_6D_6$): 8.59 (pseudo-quartet, $^4J_{HP}$ = 1.2 Hz, 1H, OC*H*O), 1.23 (t, $^2J_{HP}$ = 3.2 Hz 18H, 2$PMe_3$ trans); 1.09 (d, $^2J_{HP}$ = 6.9 Hz, 9H, $PMe_3$). $^{13}$C{$^1$H} NMR ($C_6D_6$): 230.2 (dt, $^2J_{Cpcis}$ = 11 Hz, $^2J_{CPtrans}$ = 53 Hz, CO); 167.1 (m, CHO), 17.6 (dt, $^1J_{CP}$ = 18 Hz, $^3J_{CP}$ = 3 Hz, $PMe_3$), 17.9 (td, $^1J_{CP}$ = 11 Hz, $^3J_{CP}$ = 1 Hz, 2$PMe_3$ trans). $^{31}$P{$^1$H} NMR ($C_6D_6$): −8.3 (d, $^2J_{PP}$ = 28 Hz, 2$PMe_3$ trans), −15.6 (t, $^2J_{PP}$ = 28 Hz, $PMe_3$). EI-MS: 427 (8, $M^+$), 399 (25, [$M^+$ − CO]), 397 (13, [$M^+$ − NO]), 353 (42, [$M^+$ − NO − OCHO], 323 (62, [$M^+$ − CO − $PMe_3$]), 321 (55, [$M^+$ − NO − $PMe_3$]), 278 (62, [$M^+$ − CO − OCHO − $PMe_3$]). Anal. Calcd for $C_{11}H_{28}MoNO_4P_3$: C 30.92, H 6.62, N 3.28. Found: C 31.22, H 6.72, N 3.35.

**Reaction of 3 with CO, Formation of Mo(CO)$_2$(H)(NO)(PMe$_3$)$_2$ (6).** This reaction was carried out in an NMR tube and monitored by NMR. A 0.0274 g (0.072 mmol) sample of **3** was dissolved in about 0.7 mL of $C_6D_5CD_3$ in an NMR tube. The solution was frozen, and the NMR tube was evacuated and then filled with CO (1 bar). The tube was sealed, the reaction mixture was allowed to warm to room temperature, and NMR spectra were recorded frequently. The reaction reached balance within 2 days. $^1$H NMR of **6** ($C_7D_8$): 1.12 (t, $^2J_{HP}$ = 3.2 Hz, 18H, 2$PMe_3$); −2.73 (t, $^2J_{HP}$ = 29.6 Hz, 1H, Mo−H). $^{31}$P{$^1$H} NMR ($C_7D_8$): −6.5 (s).

**Preparation of *mer*-Mo[($\mu$-OCH)Fe(CO)$_4$](CO)(NO)(PMe$_3$)$_3$ (7a).** A mixture of 0.065 g (0.17 mmol) of **3** and 23 $\mu$L (0.17 mmol) of $Fe(CO)_5$ in 6 mL of toluene was stirred at rt for 1 h. After this time the solvent was evaporated in vacuo and the residue was extracted with pentane. Concentration and chilling of the combined solutions to −30 °C afforded yellow crystals of **7a**. Yield: 0.0862 g (88%). IR ($cm^{-1}$, THF): 2035, 1952, 1925 ($Fe(CO)_4$), 1931 (Mo(CO)), 1619 (NO). $^1$H NMR ($C_6D_6$): 14.09 (s, 1H, OCH), 1.00 (t, $^2J_{HP}$ = 1.6 Hz, 18H, 2$PMe_3$ trans); 1.02 (d, $^2J_{HP}$ = 2.0 Hz, 9H, $PMe_3$). $^{13}$C{$^1$H} NMR ($C_6D_6$): 228.5 (dt, $^2J_{CPcis}$ = 11 Hz, $^2J_{CPtrans}$ = 48 Hz, Mo−CO); 306.1 (pseudo-quartet, $^3J_{CP}$ = 3 Hz, $^3J_{CPtrans}$ = 2 Hz, −OCH−), 218.2 (s, $Fe(CO)_4$), 16.7 (dt, $^1J_{CP}$ = 20 Hz, $^3J_{CP}$ = 3 Hz, $PMe_3$), 17.1 (td, $^1J_{CP}$ = 12 Hz, $^3J_{CP}$ = 1 Hz, 2$PMe_3$ trans). $^{31}$P{$^1$H} NMR ($C_6D_6$): −9.9 (d, $^2J_{PP}$ = 27 Hz, 2$PMe_3$ trans), −15.6 (t, $^2J_{PP}$= 27 Hz, $PMe_3$). EI-MS: 551 (10, [$M^+$ − CO]), 549 (10, [$M^+$ − NO]), 503 (24, [$M^+$ − $PMe_3$]), 382 (12, [$M^+$ − OCH$Fe(CO)_4$]), 354 (26, [$M^+$ − CO − OCH$Fe(CO)_4$]), 278 (30, [$M^+$ − CO − OCH$Fe(CO)_4$ − $PMe_3$]). 196 (100, $Fe(CO)_5$), 168 (100, $Fe(CO)_4$). Anal. Calcd for $C_{15}H_{28}FeMoNO_7P_3$: C 31.11, H 4.88, N 2.42. Found: C 31.28, H 4.58, N 2.30.

**Preparation of *mer*-Mo[($\mu$-OCH)Re$_2$(CO)$_9$](CO)(NO)(PMe$_3$)$_3$ (7b).** A mixture of 0.060 g (0.16 mmol) of **3** and 0.105 g (0.16 mmol) of $Re_2(CO)_{10}$ in 10 mL of toluene was stirred for 1 h at rt. After this time the solvent was removed in vacuo. The residue was extracted with $Et_2O$, and the combined solutions were concentrated and cooled to −30 °C to afford orange crystals of **7b**. Yield: 0.130 g (80%). IR ($cm^{-1}$, Nujol): 2094, 2030, 2014, 1984, 1955, 1918, 1908 ($Re_2(CO)_9$), 1932 (Mo−CO), 1618 (NO). $^1$H NMR ($C_7D_8$): 15.07 (s, 1H, OC*H*), 1.06 (t, $^2J_{HP}$ = 3.2 Hz, 18H, 2$PMe_3$ trans); 0.95 (d, $^2J_{HP}$ = 7 Hz, 9H, $PMe_3$). $^{13}$C{$^1$H} NMR ($C_7D_8$): 288.3 (dt, $^2J_{CPcis}$ = 10 Hz, $^2J_{CPtrans}$ = 49 Hz, Mo−CO); 302.3 (pseudo-quartet, $^3J_{CP}$ = 4 Hz, OCH), 200.9, 196.5, 191.9 (3s, $Re_2(CO)_9$), 16.9 (dt, $^1J_{CP}$ = 20 Hz, $^3J_{CP}$ = 3 Hz, $PMe_3$, 17.5 (td, $^1J_{CP}$ = 12 Hz, $^3J_{CP}$ = 1 Hz, 2$PMe_3$ trans). $^{31}$P{$^1$H} NMR ($C_7D_8$): −11.6 (d, $^2J_{PP}$ = 30 Hz, 2$PMe_3$ trans), −16.4 (t, $^2J_{PP}$ = 30 Hz, $PMe_3$). EI-MS: 797 (20, [$M^+$ − 2CO − NO − 2$PMe_3$]), 710 (30, [$M^+$ − $Re(CO)_5$]), 633 (38, [$M^+$ − $Re(CO)_5$ − $PMe_3$]), 605 (14, [$M^+$ − $Re(CO)_5$ −

$PMe_3$ − CO]), 306 (23, [$M^+$ − $OCHRe_2(CO)_{10}$ − $PMe_3$]), 278 (20, [$M^+$ − CO − $OCHRe_2(CO)_{10}$ − $PMe_3$]). Anal. Calcd for $C_{20}H_{28}MoNO_{12}P_3Re_2$: C 23.19, H 2.73, N 1.35. Found: C 23.32, H 2.57, N 1.25.

**Attempted Reactions of 3 with the Imines PhN=CHPh, MeN=CHPh, and $Ph_2C$=NH.** All reactions were carried out in an NMR tube and monitored by NMR. A 0.020 g (0.05 mmol) sample of **3** and stoichiometric amounts of the imine were dissolved in about 0.7 mL of $C_6D_5CD_3$, and the mixture was transferred into a NMR tube. The $^1$H NMR and $^{31}$P NMR spectra were recorded revealing no reaction at rt and 60 °C for MeN=CHPh and $Ph_2C$=NH. The reaction with PhN=CHPh revealed new resonances with complete transformation, which however could not be assigned to a unique species.

**Preparation of *trans*-Mo[OCH(OCH$_3$)(C$_4$H$_6$N)](CO)(NO)-(PMe$_3$)$_2$ (8).** A mixture of 0.050 g (0.13 mmol) of **3** and 22 $\mu$L (0.13 mmol) of (pyrrolidine-2-yl)methyl carboxylate in 5 mL of toluene was stirred for 2 h at rt. After this time the solvent was evaporated in vacuo and the residue was extracted with $Et_2O$. Concentration and chilling of the combined solutions to −30 °C afforded red crystals of **8**. Yield: 0.047 g (83.0%). IR (cm$^{-1}$, hexane): 1908 (CO), 1592 (NO). $^1$H NMR ($C_6D_6$): 5.41 (t, $^4J_{HH}$ = 4.7 Hz, 1H, OCH), 3.56 (br, 2H, pyrrolidine−$H_2C(5')$), 3.36 (s, 3H, −$OCH_3$), 2.43 (m,1H, pyrrolidine−HC(3′)), 2.04 (m, 1H, pyrrolidine−HC(3′)), 1.19 (dd, $^4J_{HP}$ = 1.9 Hz, $^2J_{HP}$ = 4.3 Hz, 9H, $PMe_3$), 1.03 (dd, $^4J_{HP}$ = 1.9 Hz, $^2J_{HP}$ = 4.3 Hz, 9H, $PMe_3$). $^{13}$C{$^1$H} NMR ($C_6D_6$): 244.4 (t, $^2J_{CP}$ = 10 Hz, CO); 186.3 (t, $^3J_{CP}$ = 3 Hz, C=N), 104.9 (s, −OCH−), 59.6 (s, −$OCH_3$), 53.7, 32.5, 23.1 (3s, pyrrolidine−C), 15.1 (dd, $^1J_{CP}$ = 13 Hz, $^3J_{CP}$ = 8 Hz, $PMe_3$), 14.7 (dd, $^1J_{CP}$ = 13 Hz, $^3J_{CP}$ = 8 Hz, $PMe_3$). $^{31}$P{$^1$H} NMR ($C_6D_6$): −6.1 (s, $PMe_3$), −6.2 (s, $PMe_3$). EI-MS: 434 (30, [$M^+$]), 460 (8, [$M^+$ − CO]), 330 (100, [$M^+$ − CO − $PMe_3$]), 328 (100, [$M^+$ − NO − $PMe_3$]), 300 (66, [$M^+$ − $PMe_3$ − CO − NO]), 224 (14, [$M^+$ − NO − CO − 2$PMe_3$]). Anal. Calcd for $C_{13}H_{28}MoN_2O_4P_2$: C 35.95, H 6.51, N 6.45. Found: C 36.26, H 6.03, N 6.46.

**Computational Details.** Self-consistent GGA calculations with gradient corrections due to Becke[39] and Perdew[40] have been performed utilizing the Amsterdam Density Functional package ADF.[41] Use was made of the frozen core approximation. Methyl groups were described using a double-ζ STO basis (ADF database II). For the *n*s, *n*p, *n*d, and (*n*+1)s shells on the transition metals, and for H, a triple-ζ STO basis augmented by one (*n*+1)p function was employed (ADF database IV). The valence shell of the remaining main group elements was described with a double-ζ STO basis and one d-STO polarization function (ADF database III). The numerical integration grid[42] was chosen in a way that significant test integrals are evaluated with an accuracy of at least four significant digits. Relativistic effects were included using a quasi-relativistic approach.[43] For systems with an odd electron count, spin-unrestricted calculations have been performed. The atomic reference energy for the $^2$S ground state of H was taken as 92 kJ/mol, as suggested by Baerends et al.[44] The reaction enthalpies $\Delta H$ were obtained by correcting the reaction energies $\Delta E$ for zero-point energy (ZPE). For reactions I and VIII, this contribution has been estimated as −10 kJ/mol from $\nu$(Mo−H) reported for Mo(CO)H(NO)($PMePh_2$)$_3$,[8] for reactions II, IV, VI, and VII as 20 kJ/mol from the calculated $\Delta ZPE$ between CO and HCO, and for reactions III and V as 4 kJ/mol from related $\nu$(M−O) values.[45]

**X-ray Crystal Structure Analyses on 2, 3, 4b, 7a, 7b, and 8.** X-ray diffraction data were collected at 193(1) K using an imaging plate detector system (STOE IPDS) with graphite-monochromated Mo Kα radiation. A total of 180, 143, 180, 150, 180, and 150 images were exposed at constant times of 1.50, 1.20, 1.70, 2.20, 3.00, and 1.30 min/image for **2**, **3**, **4b**, **7a**, **7b**, and **8**, respectively. The crystal-to-image distances were set to 60, 60, 50, 66, 70, and 50 mm ($\theta_{max}$ = 28.03°, 28.04°, 30.35°, 26.85°, 25.88°, and 30.34°). $\phi$-oscillation (**7b**) or rotation scan modes (**2**, **3**, **4b**, **7a**, **8**) were selected for the $\phi$ increments of 1.0°,1.4°, 1.0°, 1.0°, 1.0°, and 1.0° per exposure in each case. Total exposure times for the six compounds were 17, 13, 18, 15, 22, and 14 h in the order of the complexes as given above. The intensities were integrated after using a dynamic peak profile analysis, and estimated mosaic spread (EMS) check[46] was performed to prevent overlapping intensities. A total of 5000 reflections (8000 for **4b**) were selected out of the whole limiting sphere for the cell parameter refinement. A total of 29 126, 33 390, 31 045, 27 597, 22 695, and 30 592 reflections were collected, of which 9526, 8731, 8964, 5287, 6130, and 11 792 reflections were unique ($R_{int}$ = 5.20%, 4.06%, 4.25% 5.65%, 10.88%, and 4.34%); data reduction and numerical absorption correction used 14, 19, 17, 16, 11, and 12 indexed crystal faces.[46] All six structures were solved by the Patterson method using an improved version of SHELXS-97[47] and refined with SHELXL 97.[48] Absolute configurations were determined by using Flack's *x*-parameter refinement.[48,49] The absolute structure parameter *x* for compounds **3** and **8** was −0.03(2) and 0.04(3), respectively. No twinning by merohedry was noted for both of the non-centrosymmetric structures.

**Acknowledgment.** F.L. would like to thank the China Scholarship Council and the University of Zurich for providing an exchange scholarship. H.B. gratefully acknowledges support from the Swiss National Science Foundation and from the funds of the University of Zurich. We furthermore thank Ms. B. Spichtig for MS analyses.

**Supporting Information Available:** Tables of crystal data and structure refinement parameters, atomic coordinates, bond lengths, bond angles, anisotropic displacement parameters, and hydrogen coordinates of **2**, **3**, **4b**, **7a**, **7b**, and **8**. Optimized geometries and bonding energies for all calculated molecules. This material is available free of charge via the Internet at http://pubs.acs.org.

OM990945T



(39) Becke, A. D. *Phys. Rev. A* **1988**, *38*, 3098.
(40) Perdew, J. P. *Phys. Rev. B* **1986**, *33*, 8822.
(41) (a) Baerends, E. J.; Bérces, A.; Bo, C.; Boerrigter, P. M.; Cavallo, L.; Deng, L.; Dickson, R. M.; Ellis, D. E.; Fan, L.; Fischer, T. H. Fonseca Guerra, C.; van Gisbergen, S. J. A.; Groeneveld, J. A.; Gritsenko, O. V.; Harris, F. E.; van den Hoek, P.; Jacobsen, H.; van Kessel, G.; Kootstra, F.; van Lenthe, E.; Osinga, V. P.; Philipsen, P. H. T.; Post, D.; Pye, C. C.; Ravenek, W.; Ros, P.; Schipper, P. R. T.; Schreckenbach, G.; Snijders, J. G.; Sola, M.; Swerhone, D.; te Velde, G.; Vernooijs, P.; Versluis, L.; Visser, O.; van Wezenbeek, E.; Wiesenekker, G.; Wolff, S. K.; Woo, T. K.; Ziegler, T. *ADF Release 1999.01/02*; SCM: Amsterdam, 1999. (b) Guerra, C. F.; Snijders, J. G.; te Velde, G.; Baerends, E. J. *Theor. Chem. Acc.* **1998,** *99*, 391.
(42) te Velde, G.; Baerends, E. J. *J. Comput. Phys.* **1992**, *99*, 84.
(43) Ziegler, T.; Tschinke, V.; Baerends, E. J.; Snijders, J. G.; Ravenek, W. *J. Phys. Chem.* **1989**, *93*, 3050.
(44) Baerends, E. J.; Branchadell, V.; Sodupe, M. *Chem. Phys. Lett.* **1997**, *265*, 481.
(45) Nakamoto, K. *Infrared and Raman Spectra of Inorganic and Coordination Compounds*, 3rd ed.; John Wiley: New York, 1978; Chapter III-6.
(46) Stoe IPDS software for data collection, cell refinement, and data reduction, Version 2.87−2.92 (the latter used for **4b**); Stoe & Cie, Darmstadt, Germany, 1997−1999.
(47) SHELXS-97: Sheldrick, G. M. *Acta Crystallogr.* **1990**, *46A*, 467.
(48) SHELXL-97: Sheldrick, G. M. *Programme for the Refinement of Crystal Structures*; University of Göttingen: Germany, 1997.
(49) Flack, H. D. *Acta Crystallogr.* **1983**, *A39*, 876.
(50) Bernardinelli, G.; Flack, H. D. *Acta Crystallogr.* **1985**, *A41*, 500.